CHAPTER IV

RESULTS AND DISCUSSION

4.1 Clay preparation and characterization

4.1.1 Clay mineral identification by X-ray diffraction

For qualitative identification, the diffractogram has been searched and matched with in JCPDS powder diffraction cards. It illustrated that the as-received bentonite from Thai Nippon chemical co.,ltd. composed of clay minerals and non clay minerals, the main phase is montmorillonite and the other phases are quartz cristobalite and illite (see in Table 4.1). When it was purified by sedimentation technique, the residual of clay mineral and non clay mineral which have particle size more than 2 μm had been removed as showing in the X-ray diffractograms Figure 4.1.

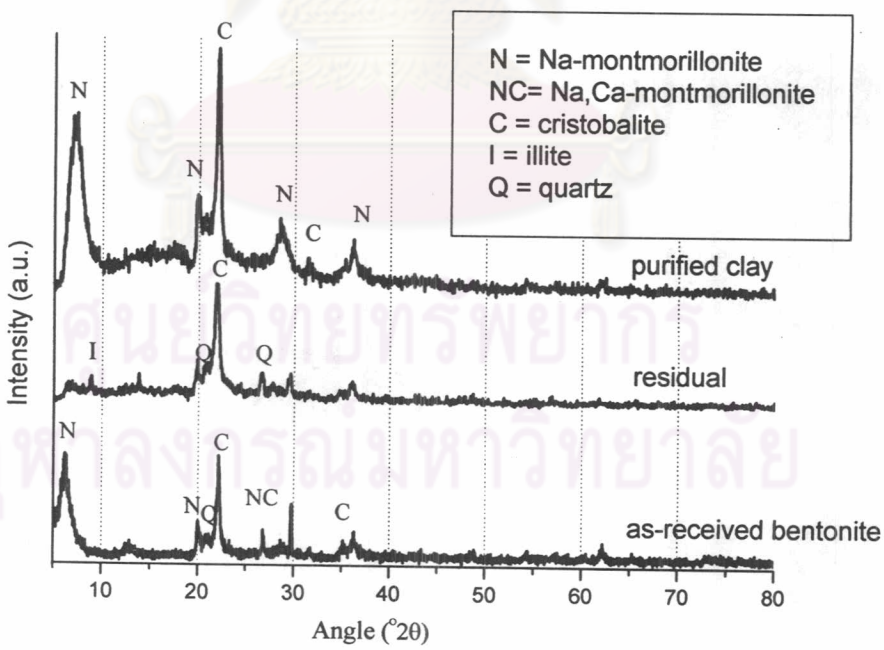

Figure 4.1 X-ray diffractograms of bentonite before and after purification.

Table 4.1 A comparison X-ray diffractogram of bentonite between before and after separation process (JCPDs No. 03-0010, 11-0695, 29-1498, and 33-1161)

As-received bentonite		Purified clay		Residual	
Angle ($^o2\theta$)	Index	Angle ($^o2\theta$)	Index	Angle ($^o2\theta$)	Index
6.28	Na-Mont.	6.95	Na-Mont.	-	-
-	-	-	-	8.75	Illite
19.85	Na-Mont.	19.85	NA-Mont.	-	-
20.75	Quartz	-	-	20.75	Quartz
22.05	Cristobalite	22.05	Cristobalite	22.05	Cristobalite
26.65	Quartz	-	-	26.65	Quartz
28.75	Na,Ca-Mont.	28.75	Na,Ca-Mont.	-	-
31.45	Cristobalite	31.45	Cristobalite	31.45	Cristobalite
35.10	Na-Mont	35.10	Na-Mont.	-	-
36.11	Cristobalite	36.11	Cristobalite	36.11	Cristobalite
54.30	Na-Mont.	54.30	Na-Mont.	-	-
62.10	Na-Mont	62.10	Na-Mont.	-	-

However this procedure could not removed all of cristobalite because its has specific gravity and particle size closed to Na-montmorillonite. In sedimentary rocks and soil, the mixed-layer clay mineral usually found such as illite/smectite, chlorite/smectite and chlorite/vermiculite. The best method to identify illite smectite and vermiculite is the comparison of x-ray diffractogram of clay mineral at air dried and ethylene glycol solvated state [Whitting, 1965 and Moore, 1997]. Smectite, expanded clay, can adsorb ethylene glycol into the interlayer as a result of the larger d_{001} spacing than air dried smectite. While ethylene glycol can not penetrate into the interlayer of Chlorite and vermiculite see in Table 4.2. The X-ray diffractograms of clay mineral from this work with different conditions have not shown the peak around 5.8-6.3 $^o2\theta$ after solvated with ethylene glycol and the peak at 6.3 $^o2\theta$ after heated at 550 ^oC. This indicates that there are not vermiculite or illite contaminant phase as shown in Figure 4.2

Table 4.2 The d_{001} spacing of clay minerals from various treatments.[Whitting, 1965]

Treatment	Position of diffraction peak ($^{o}2\theta$)	d_{001} spacing (nm)	Clay minerals
Mg-saturated air dried	5.8-6.3	1.40-1.50	smectite, vermiculite, chlorite
	8.7-8.9	0.99-1.01	mica(illite), halloysite
	11.8-12.3	0.72-0.75	metahalloysite
	12.4	0.715	kaolinite, chlorite(2^{nd} order)
Mg-saturated Ethylene glycol-solvated	4.9-5.2	1.77-1.80	smectite
	5.8-6.3	1.40-1.50	vermiculite, chlorite
	8.2	1.08	halloysite
	8.7-8.9	0.99-1.01	mica(illite)
	11.8-12.3	0.72-0.75	metahalloysite
	12.4	0.715	kaolinite, chlorite(2^{nd} order)
K-saturated air dried	5.8-6.3	1.40-1.50	chlorite, vermiculite (with interlayer aluminium)
	6.9-7.1	1.24-1.28	smectite
	8.7-8.9	0.99-1.01	mica(illite), halloysite, vermiculite(contracted)
	11.8-12.3	0.72-0.75	metahalloysite
	12.4	0.715	kaolinite, chlorite(2^{nd} order)
K-saturated heated at 550 °C	5.8-6.3	1.40-1.50	chlorite
	8.7-8.9	0.99-1.01	mica, vermiculite(contracted), smectite(contracted)
	12.4	0.715	chlorite(2^{nd} order)

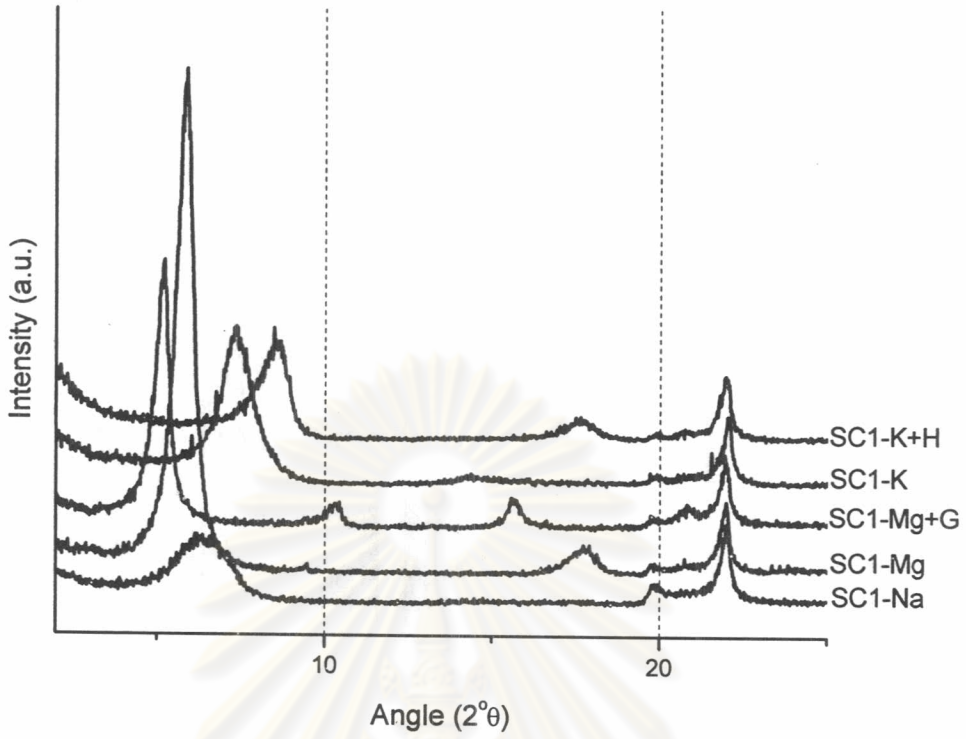

Figure 4.2 X-ray diffractograms of montmorillonite after saturated with different cations and solvated with ethylene glycol.

4.1.2 Chemical composition investigation

The chemical composition of clay mineral investigated by X-ray fluorescence is shown in Table 4.3.

Table 4.3 The chemical composition of clay

Clay	Weight of oxide (%)							
	Al_2O_3	SiO_2	Fe_2O_3	Na_2O	TiO_2	MgO	K_2O	CaO
SC1	13.30	76.65	1.48	1.57	0.28	2.60	0.59	2.92
Na-SC1	16.53	75.80	1.42	2.64	0.18	2.75	0.34	0.25

From these compositions, the formula structure of montmorillonite can be calculated as $Na_{0.75}Ca_{0.07}K_{0.07}(Al_{2.82}Mg_{1.18}Fe_{0.21})Si_8O_{20}(OH)_4$. The calculated CEC form the formula is 128 meq/100 g. of clay.

4.1.3 Determination of cation exchange capacity(CEC) by methylene blue index

The CEC of Na-montmorillonite, investigated by methylene blue index based on ASTM C837-81 (1992) is 98 meq./100 g. of clay. It is lower than the calculated CEC from the formula because the sample contains about 25-30 % cristobalite which explained by XRD semi-quantitative.

The specific surface area was calculated by the amount of methylene blue which was adsorbed on the surface of clay by taking the molecule area about 130 $Å^2$ is 774.77 m^2/g. Also the surface charge density is 1.28 x 10^{-3} meq/m^2 or 0.12 C/m^2 when 1 meq equal to 96.5 C.

The specific surface area was calculated from CEC following equation [2], Chapter 2, which was explained by Lagaly (1994), is 707.95 m^2/g. Also the surface charge density is 1.38 x 10^{-3} meq/m^2 or 0.13 C/m^2 when 1 meq equal to 96.5 C, calculated form equation [3] in Chapter 2

4.1.4 Particle size analysis

Sample, 10 %W/V swollen in deionized water, was investigated for particle size distribution by Mastersizer S Ver.2.19 with the detection range of 0.05-880.00 μm. The result is shown in Figure 4.3 which implied that the clay mineral or montmorillonite has a particle size less than 2 μm and the 90% accumulated has a diameter (D_{90}) of 0.57 μm. From this result this method was approved for the separation of the clay minerals.

The particle size distribution of sample when dispersed in ethanol, has been shown the 90% accumulated has a diameter (D_{90}) 66.69 μm. in Figure 4.4. It implied that Na-clay after drying has been aggregated. The particle size distribution depending upon the grinding process and screen by sieve. However the clay particle can be disaggregated when dispersed in water

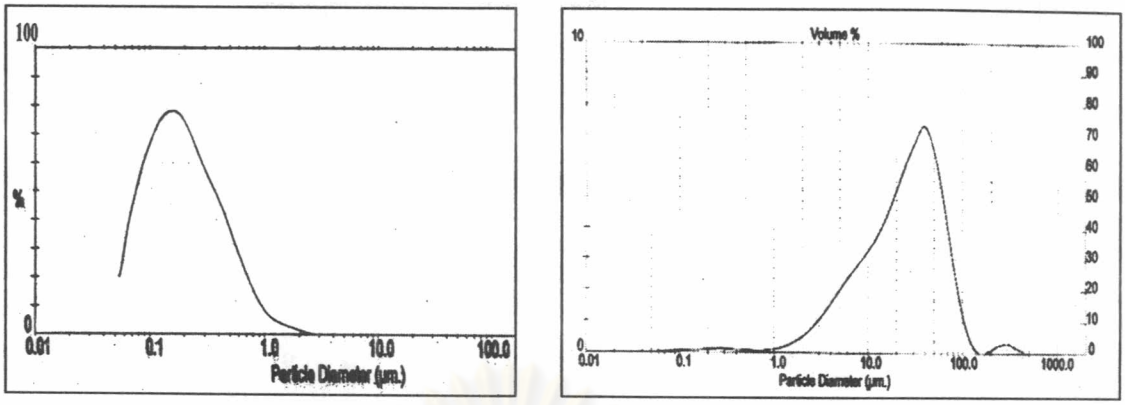

(a) (b)

Figure 4.3 Particle size distribution of Na-clay in water (a).and ethanol (b)

4.1.5 Morphology of clay mineral by SEM

The micrograph (Figure 4.4) was observed by scaning electron microscope at high magnification, showing plate-like particles less than 2 µm. This information is similar to the SEM micrograph of bentonite from Wyoming (Joann, 1984). It indicates that the clay mineral in this experiment is a smectite clay of Na/Ca montmorillonite type.

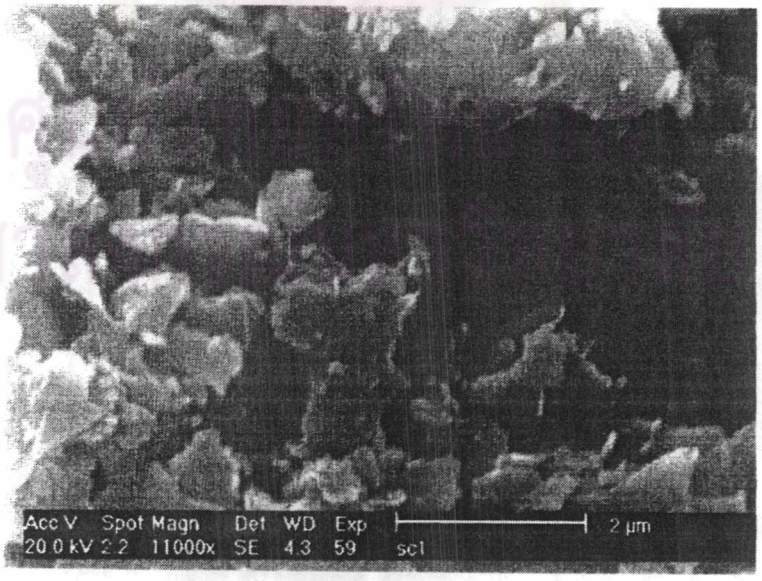

Figure 4.4 SEM image of Na-montmorillonite particle

4.2 Organoclay preparation and characterization

4.2.1 The absorption formation of S18, D18, T8 and EO18 organoclay

The main objective of this part is to engineer the surface of the clay with various types of surfactant. It is done in order to improve the organoclay affinity toward organic solvent and polymer. Four types of alkylammonium based surfactants were chosen. They are the alkylammonium ion with a single, double, and triple stranded chain. Another surfactant is the alkylammonium with the bulky ethoxy side chain. A relationship between the surfactant architecture on the absorption process was deduced via an absorption isotherm. The major differences among the surfactants are its area occupied by molecule and its chemistry. This would allow one to control the clay's surface property by simply control the absorbed surfactant on the clay layer. A degree of surface coverage has long been known to play a major role in the dispersion and wetting of a particulate object [Ishida H., 2000].

The adsorption of Na-montmorillonite was carried out in aqueous solution. The amount of alkylammonium ion loading is normalized to the clay's CEC value. The organoclay was separated by filtration and washed until free of chloride ion. Amount of the absorbed surfactant was determined by TGA. The absorption isotherm was constructed based on the relationship between the alkylammonium ion loading and the amount of the alkylammonium ions held by the clay.

Absorption of single stranded alkylammonium (S18):

Figure 4.5 shows the XRD of the organoclay prepared from a single stranded alkylammonium ion, S18, as a function of its loading.

The peak shows a gradual increase in the d-spacing as a function of loading. The increase starts leveling off after the surfactant loading has a CEC higher than 1.5 . To gain insight into the amount of the surfactant absorbed in the interlayer, the weight loss determination of the organoclay was carried out by TGA (Figure 4.6).

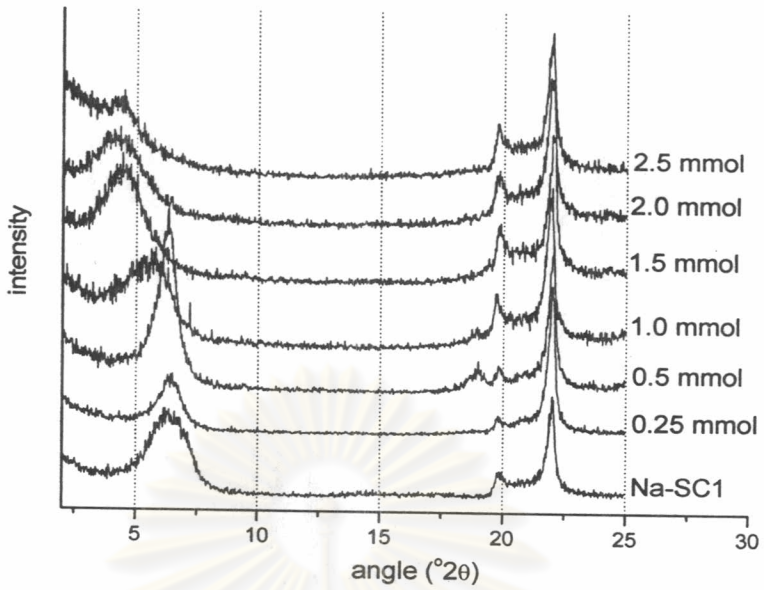

Figure 4.5 XRD of S18-SC1 organoclay as a function of S18 loading.

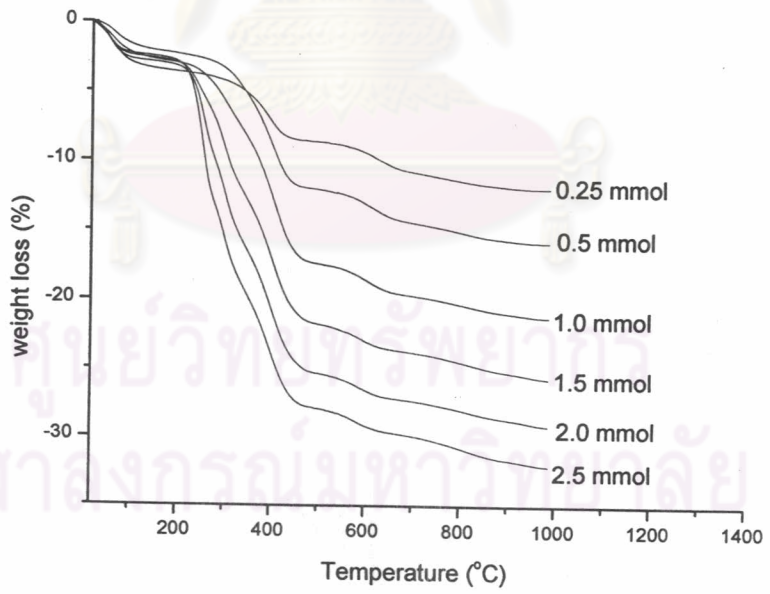

Figure 4.6 Weight loss of the S18-SC1 organoclay. The number at the end of each thermogram indicates the amount of the S18 loading.

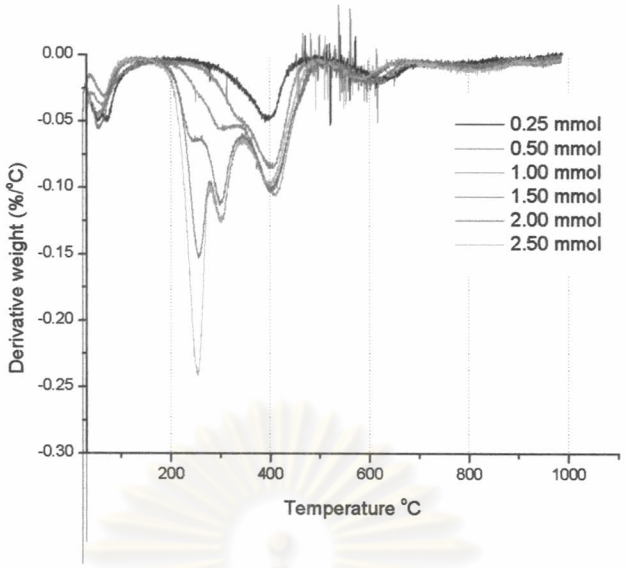

Figure 4.7 Derivative TGA plot of S18-SC1 organoclay.

In order to estimate the amount of absorbed alkylammonium, it is very important to understand the decomposition mechanism of the organoclay. The TGA can be used to reveal a degradation of mechanism of the interlayer substance within the clay. Vaia et. al. [2001] had categorized a weight loss mechanism of the organoclay into 4 regions which are

region 1. an evolution of the free water or gasneous component (at temperature below 180°C)

region 2. a decomposition of the organic substance (between 200-500 °C)

region 3. a dehydroxylation of aluminosilicate (from 500-700 °C)

region 4. a release of residual organic carboneous residue product (at 700-1000 °C).

All of the S18 organoclays show a weight loss below 100°C due to free water in Figure4.7, which resides between clay particles and adsorbs on the external surface of the clay [Xie W. et al., 2001]. Another type of water, which usually found in the clay interlayer, is as a hydrate water which is strongly associated with Na^+. It evolves at the temperature between 100-300 °C. In practice, it is very difficult to identify the strongly bonded water due to an overlapping of the peak with the loss of

surfactant [Osman M.A., 1999]. Its amount is varied inversely with the surface coverage by the surfactant within the interlayer.

An estimated weight loss of S18 organoclay at all loadings is shown in Table 4.4. The weight loss from water at low temperature and the dehydroxylation of aluminosilicate were subtracted from the total weight loss obtained from temperature between 30-800 °C.(Charles M.B.,1988).

Table 4.4 Calculated weight loss, total area occupied, and spacing for S18 intercalated montmorillonite

surfactant loading (mmol)	% weight loss		S18 loss in mmol/g of clay	% absorption efficiency	d-spacing (Å)	Δd-spacing (Å)
	Total	S18				
0	6.9	-	-	-	13.8	-
0.25	11.9	5.0	0.17	69.30	13.6	4.1
0.50	15.8	8.9	0.32	64.54	14.0	4.5
1.00	21.2	14.3	0.55	55.40	15.4	5.9
1.50	25.7	18.8	0.77	51.50	19.4	9.9
2.00	29.2	22.3	0.96	48.08	20.2	10.7
2.50	32.1	25.2	1.13	45.32	20.2	10.7

S18 loss in mmol/g of clay: This was calculated by considered only the cationic part of the S18 molecule which excludes the chloride ion. Its formula weight is 305.0 g/mol, excluded the chloride ion.

Δd-spacing (Å) = d-spacing – 9.5 Å

(a)

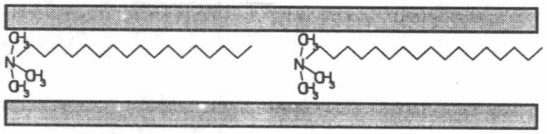

Flat lying single layer

(b)

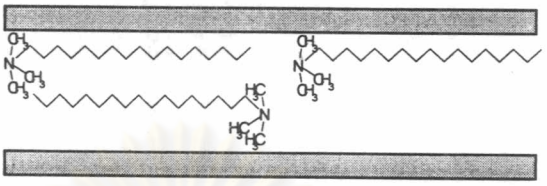

Flat lying double layer

(c)

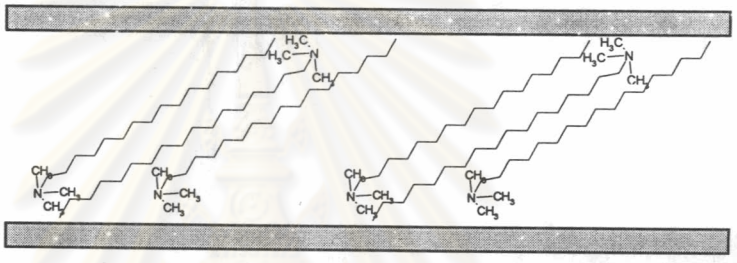

Interdigitate monolayer

Figure 4.8 Model of S18 packing in the clay interlayer

The absorption of S18 can be divided into three states depending upon the packing of the interlayer surfactants which are 1st state (initial absorption), 2nd state (transition state), and 3rd stage (complete absorption).

1st state (initial absorption): The percent of the weight loss increased as the amount of the alkylammonium ion increased. At the loading at 0.25 CEC, the d_{001} is 13.6 Å which is comparable to pure clay. TGA profile shows the first weight loss of about 3.7 % at temperature below 100 °C which corresponds to the loss of mouisture. The loss peak around 500-800 °C is the dehydroxylation of the clay which is around 3.2%. The rest of the weight loss, 5.0 %, originates from the decomposition of the S18 organic cation. There may be some of weight loss originated from tightly bound water; however, it is difficult to quantify. This amount of water is inversely proportional to the degree of the surface coverage. It will be considered that most of the weight loss is originated from the decomposition of S18 molecule. This would

give the total amount of the absorbed S18 to be 0.18 mmol. An expansion of the interlayer spacing due to the S18, Δd-spacing, is around 4.1 Å which is about the cross section of the S18 molecule. This corresponds to the flat lying of the S18 molecules on the clay surface [Lagaly G., 1986]. A similar result was observed for the higher loading, 0.50 mmol. The DTG peak is very similar to the case of 0.25 mmol surfactant loading but with the total absorption of 0.36 mmol. The S18 molecule is still lying flat on the clay surface.

2nd state (transition state): The Δd-spacing is increased to 5.9 Å with the weight loss of 14.3 % when the surfactant loading is at 1.0 CEC. The amount of the absorbed S18 is at 0.55 mmol. The ratio of the absorbed surfactant to loaded surfactant is lower, to 55.4%, when compared to the lower surfactant loading. This may suggest that there is a change in the absorption mechanism. This is consistent with the change in the interlayer spacing to 5.9 Å. A peak around 300 °C in the DTG starts to evolve which is believed to be due to a loss of a new phase of interlayer surfactant.(Osman M.A., 1999) At the loading of 1.5 mmol, the Δd-spacing is increased to 19.4 Å and the amount of absorbed alkylammonium is increased to 18.8 %. This is equivalent to 0.77 mmol of the absorbed S18 or 51.5% of absorption efficiency. The change of the Δd-spacing due to S18 is at 9.9 Å. The newly evolved peak in the DTG at 300 °C become even more prominent. The packing of the interlayer S18 is gradually transformed into the flat lying double layers (model (b), Figure 4.8) but the surface of the clay has not yet fully covered with double layer of flat lying S18 molecule. It is possible that the surfactant may present as an island of the interdigitate monolayer (model (c), Figure 4.8).

3rd state (complete absorption): The Δd-spacing remains the same at 10.7 Å for both 2.0 and 2.5 mmol loading with an increase of the total weight loss from 22.3% (0.73 mmol) to 25.2% (1.13 mmol). They correspond to the percent absorption efficiency of 48.1% and 45.3% respectively. A peak in DTG at around 300 °C due to the weight loss of newly form S18 becomes more prominent. The amount of the absorbed S18 surfactant already exceeded the CEC of clay, 98 mmol/100g of clay. At the higher loading, the amount of the absorbed surfactant is higher than the CEC of the clay. This suggests that there should be some of the physisorbed S18 present along within the interlayer. The physisorbed S18 may already presents at a lower

loading where it situates within the island of S18 molecule (if model (c) is assumed). It is possible because the charge distribution of the clay is known to be inhomogeneous. The Δd-spacing is remains the same at 10.9 Å. This would leave the only possibility that the additional surfactants are filled in the empty space within the interlayer (Figure 4.8). This is consistent with the percent efficiency of the absorption, which are comparable at 48.1% and 45.3%. The peak due to the weight loss of the new phase is become even more prominent as the surfactant loading is increased.

The other possibility, which may have an effect on the absorption, is the formation of supramolecular structure by the S18 molecule because absorption was done at the surfactant loading higher than critical micelle concentration, CMC. At the concentration higher than CMC, it is known that the alkylammonium can form the supramolecular structure eg. bilayer, vesicle [Shinoda K.,1963]. These supramolecular structures may have a direct effect on the absorption mechanism. The loading at the concentration higher than 2.50 mmol is not possible due to a limited solubility of the S18 molecule. One should take into account the solvent system used in this study because it may effect on the solubility and the supramolecular structure formed within the solution.

Absorption of D18 surfactant

The absorption of D18 surfactant can be divided into 2 states which are 1st stage (initial absorption or nucleation) and 2nd state (growth). This was judged based on the evidences from XRD, TGA, and DSC as present in Figure 4.9, 4.10, 4.11, 4.12 and Table 4.5

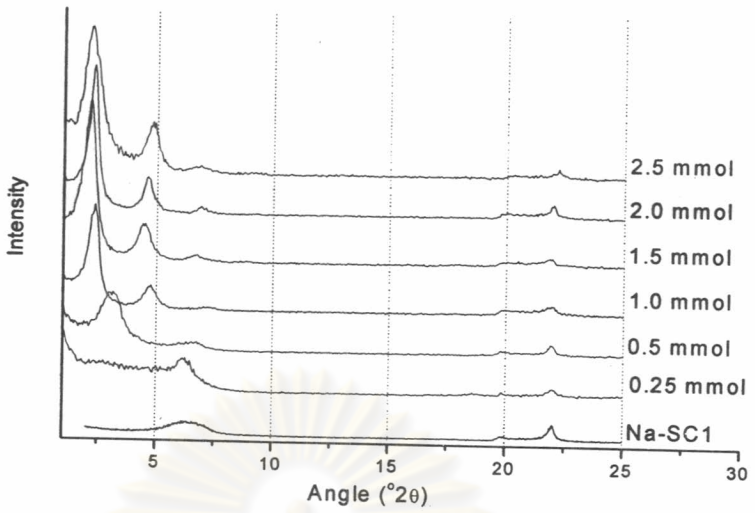

Figure 4.9 XRD of D18-SC1 organoclay as a function of D18 loading.

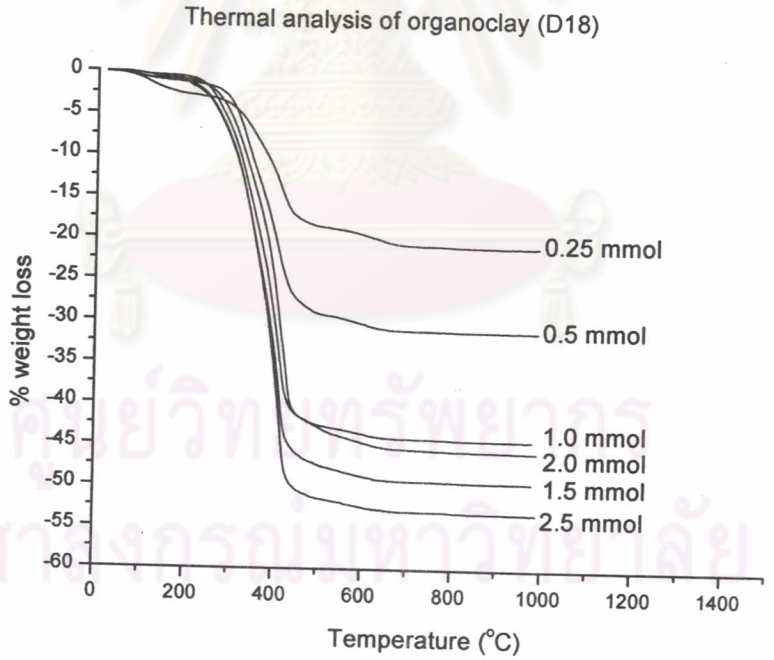

Figure 4.10 Weight loss of the D18-SC1 organoclay. The number at the end of each thermogram indicates the amount of the D18 loading.

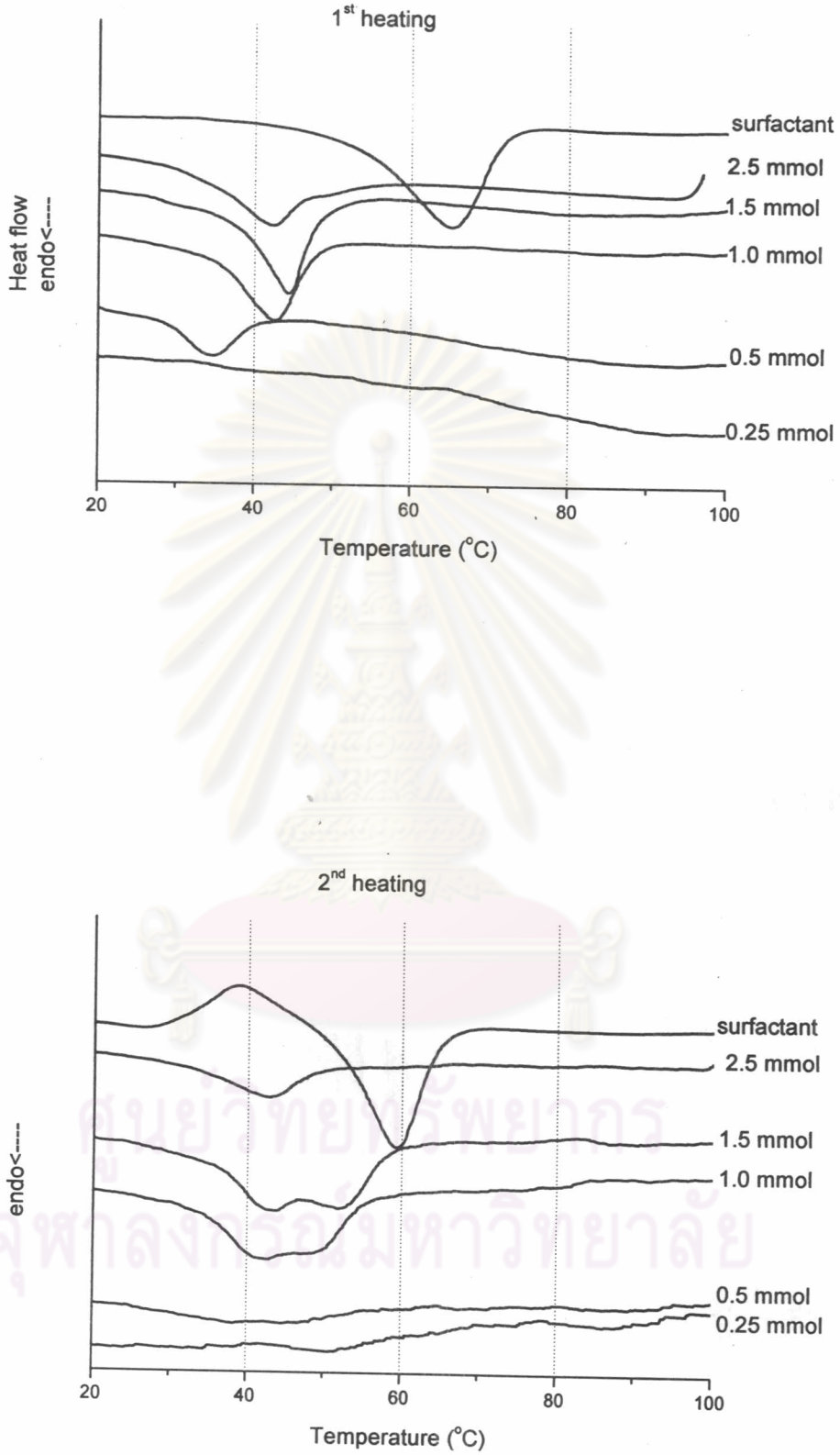

Figure 4.11 DSC plot of D18-SC1 organoclay at 1st and 2nd heat.

1st state (initial absorption or nucleation): The loading was started at 0.25 CEC, XRD shows a mixed phase of the organoclay which originates from a non uniform intercalation of the D18 into the clay interlayer. A small amount of the free water, around 3.7% was detected where the weight loss 14.0% from the D18 after taking of 3.2% of weight loss due to the dehydroxylation of the clay. An observed d-spacing is 14.2 Å which corresponds to a change in the interlayer of 4.7 Å. This corresponds to the flat lying of the surfactant D18 molecule on the surface. There is another component of the D18 molecules which are tilted with respect to the clay surface. The absorption efficiency is 100%. This suggests that the water may be absorbed along with the D18 molecules.

Table 4.5 Calculated weight loss, total area occupied, and spacing for D18

surfactant loading (mmol)	% weight loss		D18 loss in mmol/g of clay	absorption efficiency (%)	d-spacing (Å)	Δd-spacing (Å)
	Total	D18				
0	6.9	-	-	-	13.8	-
0.25	20.9	14.0	0.31	100.0	14.2	4.7
0.50	31.2	24.3	0.61	100.0	26.4	16.9
1.00	44.4	37.5	1.17	100.0	37.1	27.6
1.50	49.5	42.6	1.46	97.5	39.2	29.7
2.00	45.9	39.0	1.25	62.4	38.0	28.5
2.50	53.3	46.4	1.72	68.7	37.8	28.3

D18 loss in mmol/g of clay: This was calculated by considered only the cationic part of the D18 molecule which excludes the chloride ion. It formula weight is 537.5 g/mol)

Δd-spacing (A°) = d-spacing – 9.5 A°

The Δd-spacing is increased to 16.9 Å with the weight loss of 24.3 % at 0.5 mmol D18 loading. This is equivalent to increase of 16.9 Å due to the D18 molecules. The packing of the D18 molecules in the interlayer can be either an island of interdigitate monolayer or an island of highly tilted bilayers (Figure 4.13). This implies that D18 molecules have a denser packing than in the S18 counterpart. The special characteristic of intercalated D18 is the fact that the DSC peak can be observed in this sample (Figure 4.11). The endothermic peak in the DSC was observed in the first heating of 0.5 mmol loading. This suggests that the packing should be almost the island-like because the clay surface is not fully covered by the D18 molecules at this loading. This peak was not observed in the second heating due to the rearrange of the D18 after heating. The absorbed water is believed to be presented within the interlayer and play roles in the rearrangement of the D18. Both 0.25 mmol and 0.50 mmol loading also show a similar weight loss profile by DTG, Figure 4.12.

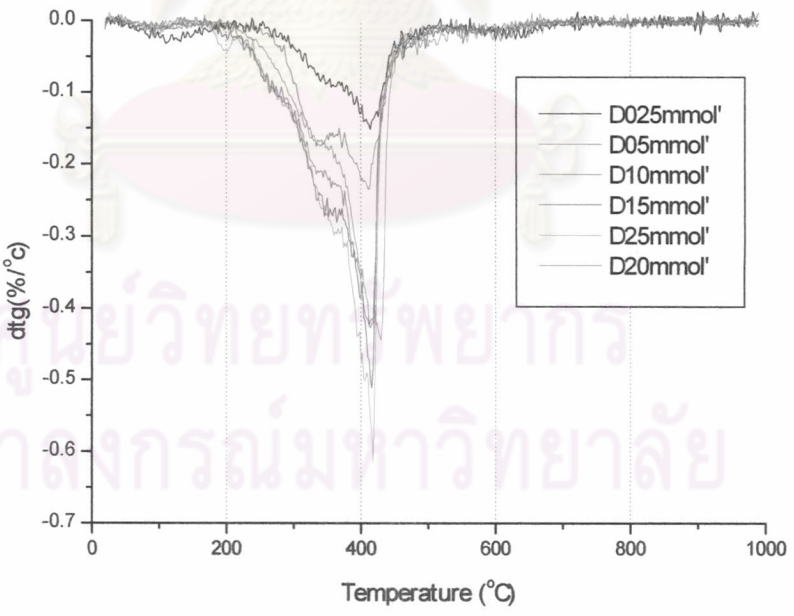

Figure 4.12 Derivative TGA plot of D18-SC1 organoclay.

2nd state (growth): The major characteristic for this state is the fact that the D18 already form the island-like packing on the clay surface. However, the surface has not yet fully covered with the D18 molecules. This would leave an empty space around the island where the hydrate water-Na^+ is located. As the amount of the alkylammonium loading is increased to 1.0 CEC, the higher weight loss (37.5%) and the increase in the Δd- spacing (27.6 Å) were observed. The spacing is larger than the length of the alkylammonium molecules; therefore, the possibility of forming the interditate monolayer packing can be excluded. This would leave only the most likely possibility which is the tilted bilayer. The absorption efficiency remains at 100%. This suggests that some water still presents in space surrounded the island of the surfactant. The DSC is further supported the dense packing of the surfactant because the endothermic peak is observed. As the surfactant loading is increased, they are merely leaving less of the empty space between the island. This is consistent with an unchanged of Δd-spacing as the D18 loading is increased. The DTG (Figure 4.12) shows a similar profile in the weight loss (at the surfactant loading higher than 1.0 mmol).

The D18 is more effective in modifying the clay surface than S18 counterpart. As evidenced by the higher absorption efficiency which is resulting in a higher surface coverage. This may be due to an intermolecular interaction of D18 which induces a closed packing.

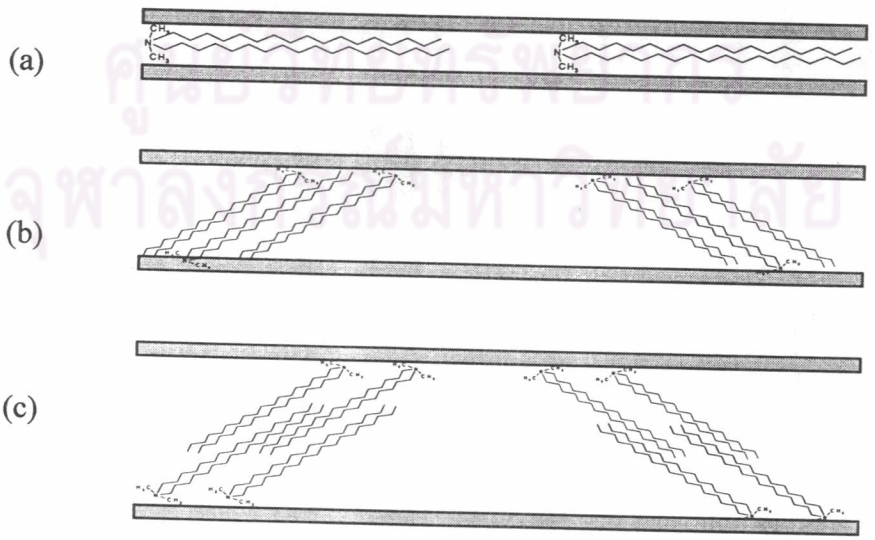

Figure 4.13 Model of D18 packing in the clay interlayer

The absorption of Aliquat (T8)

This surfactant represents the molecule with a triple in its area occupied per molecule. The absorption of T8 is similar to D18. No peak can be detected by the DSC. This may be due to a nature of T8 molecule which is relative short, only 8 carbons where the lateral packing cannot be induced. Two distinct states of packing are observed in this case.

1st state (initial absorption): The XRD and the weight loss of the T8 organoclay are shown in the Figure 4.14 and Table 4.6. At the loading of 0.5 mmol, the Δd-spacing of the organoclay is 10.7 Å with the weight loss of 13.2% (Figure 4.15). There is a small amount of the free water absorbed in the interlayer. The packing may be the flat lying bilayer or interdigitate monolayer. The absorption efficiency is 98.0%.

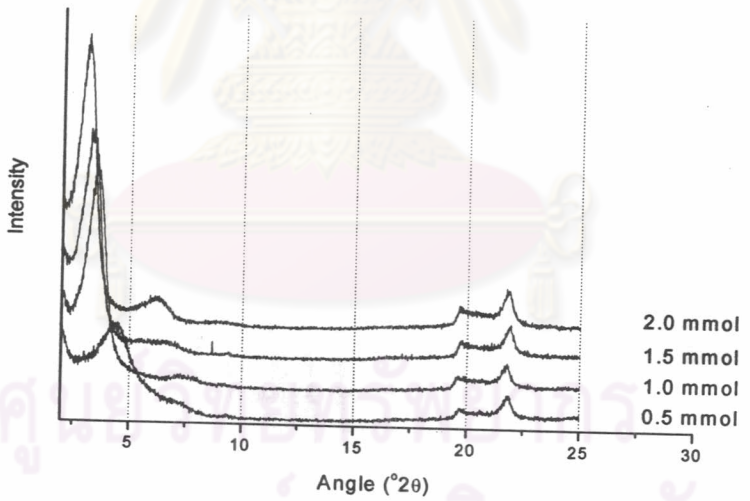

Figure 4.14 XRD of T8-SC1 organoclay as a function of T8 loading

2nd state (increase in coverage): As the amount of the surfactant is increased to 1.0 mmol, the weight loss is increased to 20.7% with the Δd-spacing of 15.4 Å. There is a gradual increase in both the observed Δd-spacing and the amount of the absorbed T8 as its loading is increased. The Δ d-spacing is increased to 17.8,

and 19.4 Å for the loading of 1.5, and 2.0 mmol loading. No extraneous effect of the interlayer water was observed in this case due to the high coverage of the surfactant. It is possible that the surfactant is not growing in the island-like manner in the case of T8 due to the lack of intermolecular interaction. The T8 molecule packs closer as the loading is increased and force the molecules to more closer and become less tilt with respect to the surface. This is the reason why the gradual change in the interlayer is observed in this case. The DTG also shows a similar profile for all the surfactant loadings in this state (Figure 4.16). The absorption efficiency is gradually decreased as the surfactant loading is increased. However they still show the most coefficient in modifying the surface when compared to S18 and D18.

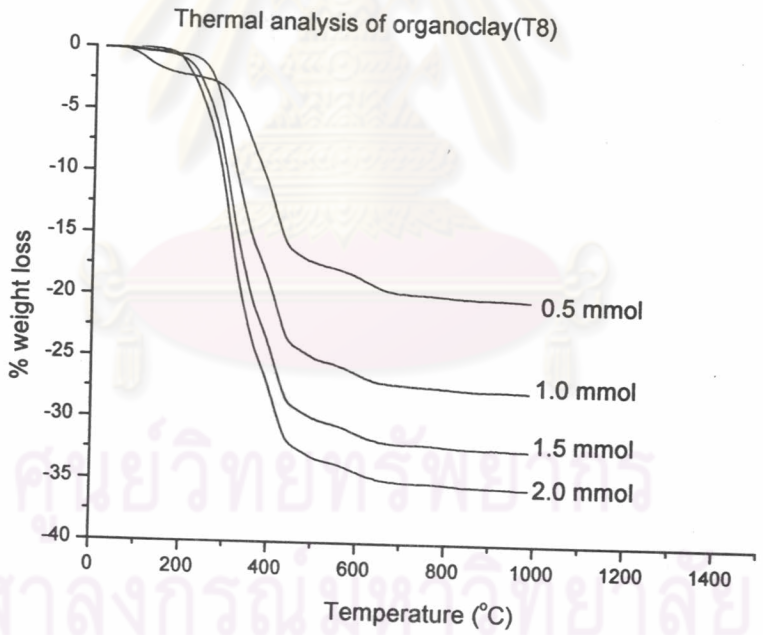

Figure 4.15 Weight loss of the T8-SC1 organoclay. The number at the end of each thermogram indicates the amount of the T8 loading.

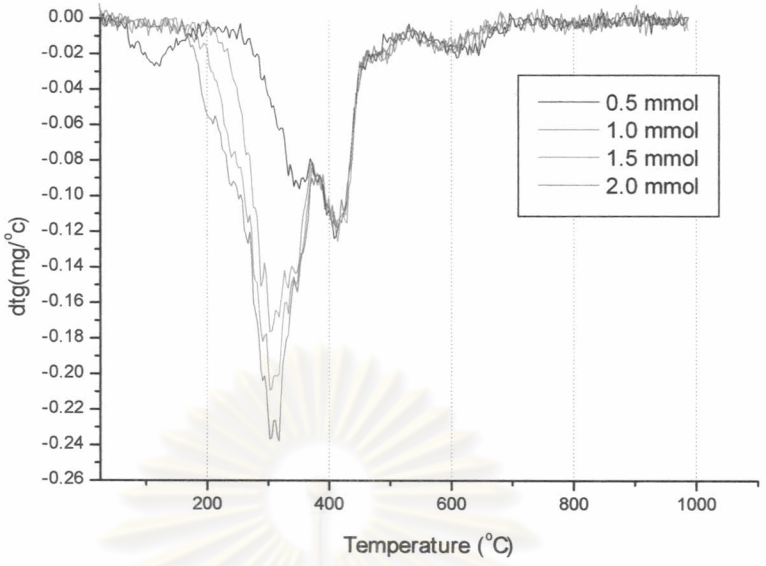

Figure 4.16 Derivative TGA plot of T8-SC1 organoclay.

Table 4.6 Calculated weight loss, total area occupied, and d-spacing for T8.

surfactant loading (mmol)	% weight loss		T8 loss in mmol	absorption efficiency (%)	d-spacing (Å)	Δd-spacing (Å)
	Total	T8				
0.50	20.1	13.2	0.42	83.5	20.2	10.7
1.00	27.6	20.7	0.72	72.2	24.9	15.4
1.50	32.5	25.6	0.96	63.9	27.3	17.8
2.00	35.5	28.6	1.12	56.0	28.9	19.4

T8 loss in mmol/g of clay: This was calculated by considered only the cationic part of the T8 molecule which excludes the chloride ion. It formular weight is 368.67 g/mol)

Δd-spacing (A^o) = d-spacing – 9.5 Å

The absorption of Ethoquad 18/25 (EO18)

EO18 represents the surfactant with the highest area occupied per molecules due to the bulky flexible ethoxy side group. The experiment is rather difficult to perform because it has a limited solubility in water.

At the initial loading of 0.5 mmol, the EO18 molecule already form a tilted bilayer with Δd-spacing of 28.7 Å. The EO18 is believed to pack as the bilayer in the island-like morphology. The ethoxy side group is not flexible as originally assumed but it is packed side by side with the C18 part. The higher loading of EO18 shows an evidence of filling the void between the island as the loading is increased to 1.0 mmol. DTG further suggests the possibility of two distinct characters of the packing depending upon the surface coverage. One was observed at the lower loading, 0.05 mmol, and the rest at the higher loading, 1.0 mmol. This is believed to be due to the difference in the packing of the surfactant in the interlayer. A further increase in the loading, all the results are inconsistent due to the limited solubility of the EO molecules in water.

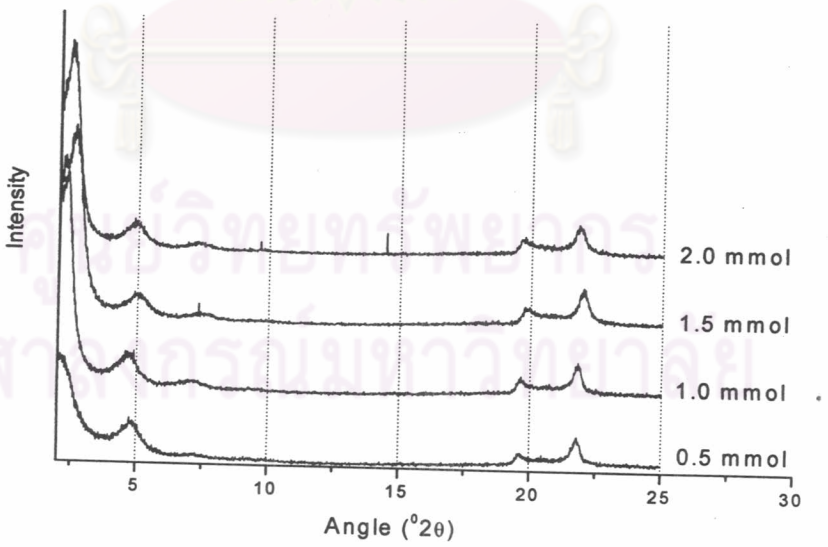

Figure 4.17 XRD of EO18-SC1 organoclay as a function of EO18 loading

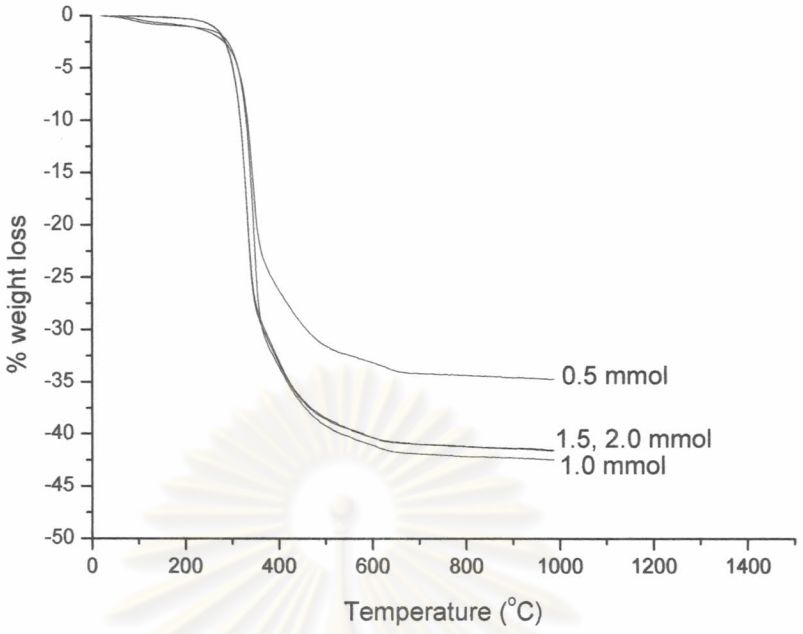

Figure 4.18 Weight loss of the EO18-SC1 organoclay. The number at the end of each thermogram indicates the amount of the EO18 loading.

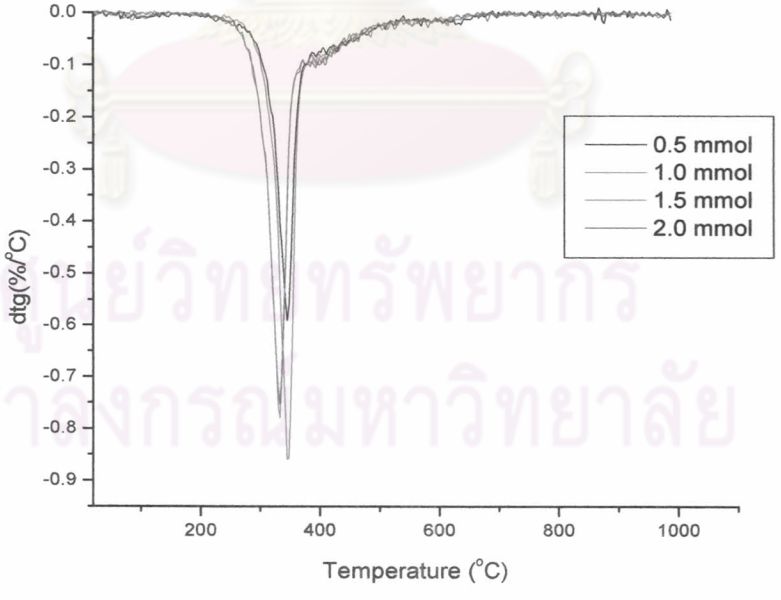

Figure 4.19 Derivative TGA plot of EO18-SC1 organoclay.

Table 4.7 Calculated weight loss, total area occupied, and spacing for EO18.

surfactant loading (mmol)	% weight loss		EO18 loss (mmol/g)	absorption efficiency (%)	d-spacing (Å)	Δd-spacing (Å)
	Total	EO18				
0.50	34.8	27.9	0.42	84.41	38.2	2.9
1.00	42.5	35.6	0.61	61.07	37.2	2.8
1.50	41.6	34.7	0.59	39.07	34.6	2.5
2.00	41.6	34.7	0.59	29.30	34.6	2.5

EO18 loss in mmol/g of clay: This was calculated by considered only the cationic part of the EO18 molecule which excludes the chloride ion. It formula weight is 944.0 g/mol)

Δd-spacing (Å) = d-spacing – 9.5 Å

4.2.2 Effect of washing on the organoclay

This experiment was done in order to elucidate the exact amount of the interlayer surfactant and the effect of the surfactant on the washing process. After the reaction with ammonium salt, the organoclay was washed with water. The washing process was carried until no white precipitate was detected with $AgNO_3$ solution. This indicates that there is no residual chloride ion, from alkylammonium salt, presence in the sample. Table 4.8 shows a comparison between the d_{001} spacing of unwahsed and chloride-free organoclay for the system of S18 and D18. A change in the interlayer spacing was detected after the washing. This implies that there is a change in the packing of the cationic surfactant within the clay layer. Two distinct features, depending upon the surfactant loading, were detected in this case. When the amount of surfactant loading is lower than the CEC, an expansion of the interlayer spacing was found. If the surfactant loading is higher than CEC, the contraction of the spacing is detected. This may be due to the nature of the absorption process and the packing of the surfactant within the interlayer.

Table 4.8 Effect of washing condition on d spacing of organoclay

concentration	d spacing of organoclay (Å)			
	S18		D18	
	Cl^-	Free Cl^-	Cl^-	Free Cl^-
0.5	13.9	14.3	28.9	32.3
1.0	15.4	14.9	37.6	34.8
1.5	20.2	18.5	41.1	36.3
2.0	20.4	18.9	38.4	37.9

At the surfactant loading lower than the CEC, 0.5 CEC, the expansion of the interlayer spacing was observed. This expansion is believed to be associated with a hydration of an un-exchanged Na^+ which presence along with the cation exchanged alkylammonium within the interlayer. As the organoclay is washed, the Na^+ is hydrated and caused the interlayer to expand. This further supports the idea of island-like absorption of the surfactant during the cation exchange reaction.

At the higher surfactant loading, the absorbed surfactant is believed to contribute cation exchange and physical absorption. The cation exchanged surfactant is bounded tightly within the interlayer by the ionic interaction. The physical absorption can be leached away by the solvent. This is resulting in the contraction of the interlayer spacing. The experiment further supports this hypothesis.

Once the surfactant is exceed 2.5 mmol, the absorption trend was reversed. This may be due to the nature of the self-assembly of the surfactant which effects the absorption.

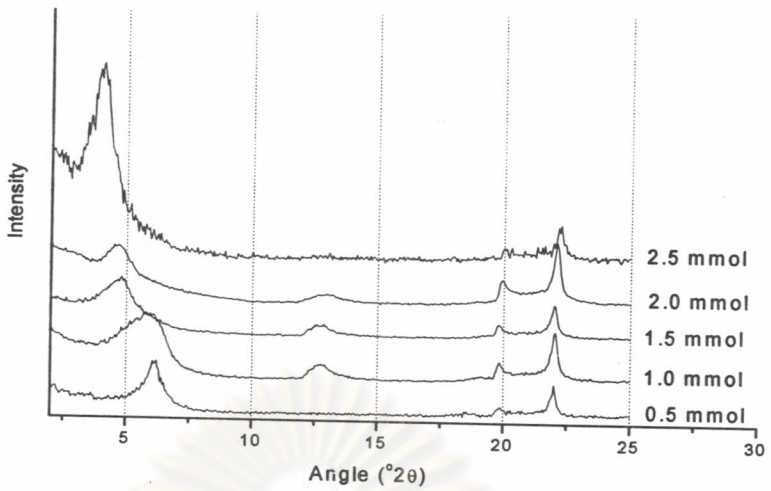

Figure 4.20 XRD of S18-SC1 organoclay as a function of S18 loading and wash until Cl^- free

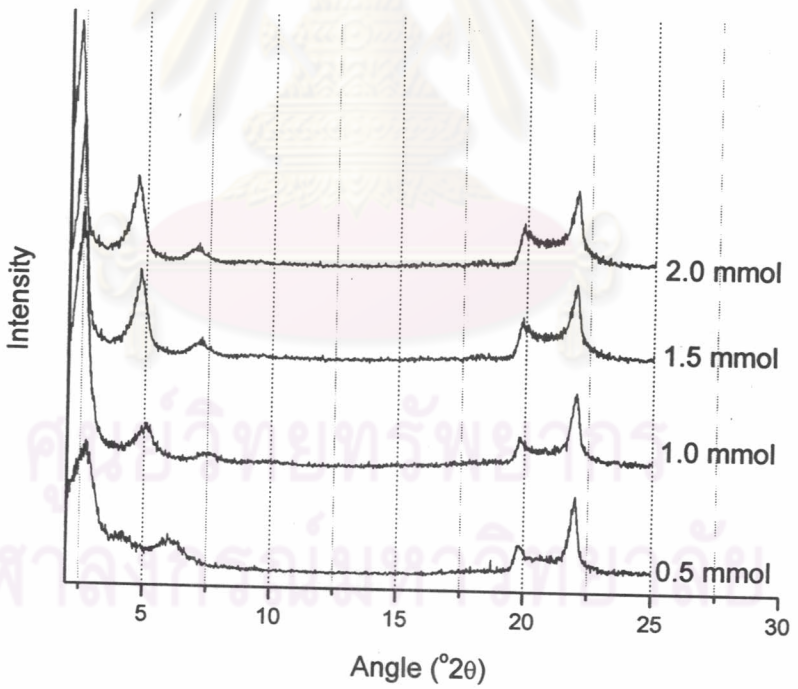

Figure 4.21 XRD of D18-SC1 organoclay as a function of D18 loading and wash until Cl^- free

If the clay with the surfactant loading is higher than CEC is washed with the good solvent, the remaining of the intercalated surfactant are comparable regardless of initial loading of the surfactant.

This hypothesis was further confirmed by the TGA experiment. 1.0 CEC D18 was picked for this experiment. Ethanol, as a good solvent for alkylammonium, was chosen for the washing process. Two washing treatments were applied to organoclay which are washed with warm EtOH and refluxed with EtOH for one day. The absorbed alkylammonium should respond to the washing process differently depending upon the mechanism of the binding. The physisorbed surfactant should be washed away while the tightly bound surfactant should remain within the interlayer. Both washing shows a comparable d-spacing and the amount of the tightly bound alkylammonium molecule. The physisorbed alkylammonium can be get rid off by successive washings the organoclay with the EtOH. This result was further confirmed by the experiment with 2.5 CEC D18 where a similar result was observed. This can be concluded that the left over surfactant is indeed the tightly bound molecule. This value is leveling off at around 28% regardless of the initial preparation condition (Table 4.9).

Table 4.9 d_{001}spacing and %weight loss of organoclay D18 (1.0 and 2.5 mmol) at various treatments

Condition	d_{001}spacing (Å)	weight loss	
		%	mmol/g
Unwashed (1.0 mmol)	37.6	37.54	1.17
washed EtOH (1.0 mmol)	31.7	26.20	0.68
Refluxed EtOH (1.0 mmol)	31.1	28.10	0.75
Refluxed EtOH (2.5 mmol)	30.9	28.80	0.78

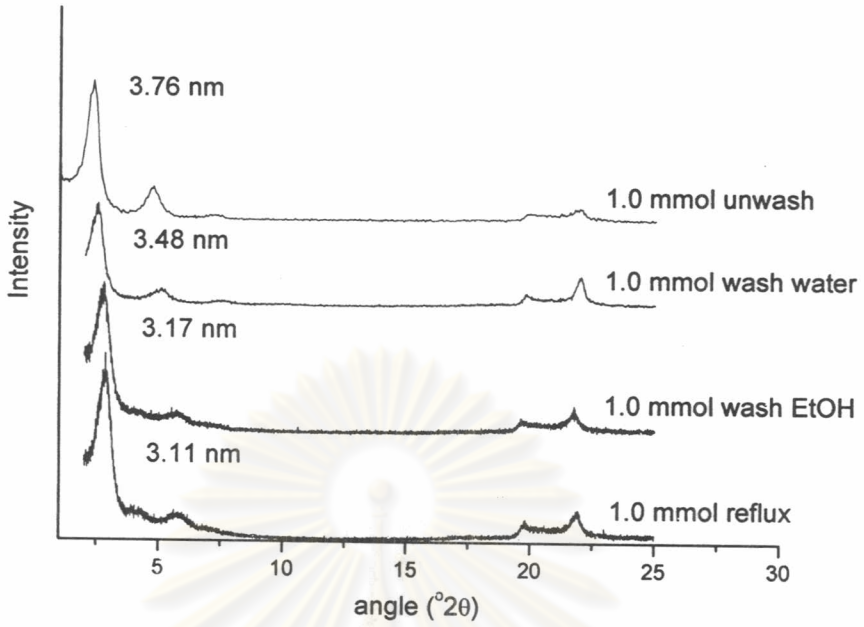

Figure 4.22 XRD pattern of organoclay D18 at various treatments.

4.3 Silane reaction and characterization

The second concept in treating the surface of the clay is by reacting the free hydroxy group of the organoclay with the silane coupling agent. This was done in order to shield the edge of the clay to reduce the electro-static interaction between the clay, thus prevent the aggregation of the clay particle. This will lead to a lower viscosity when the organoclay is used as the surfactant modifier. [Lagaly G. 2003]

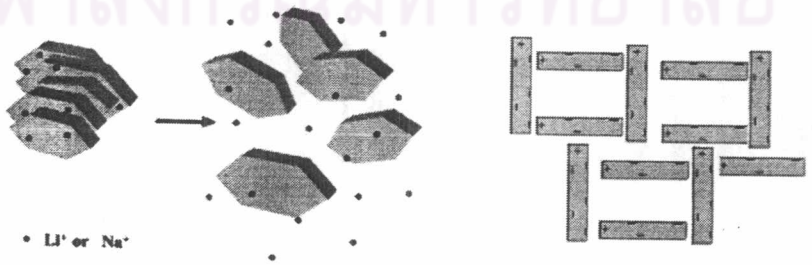

Figure 4.23 delamination of Na-montmorillonite in aqeous solotion

Octadecyl trimethoxysilane (OTMS) and octadecyl dimethychlorosilane (ODCS), a coupling agent, were used in this study. Their major difference is in their chemical structure and their interaction to the surface.

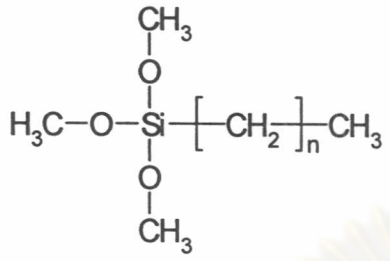

Octadecyl trimethoxy silane (OTMS)

n = 17

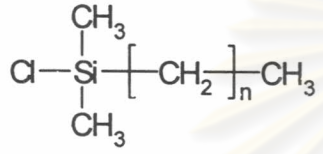

Octadecyl dimethyl chloro silane (ODCS)

n = 17

The OTMS consists of 3 reaction sites with the clay surface while the ODCS consists of one reacting site. The reaction mechanism for both ODCS and OTMS are shown below.

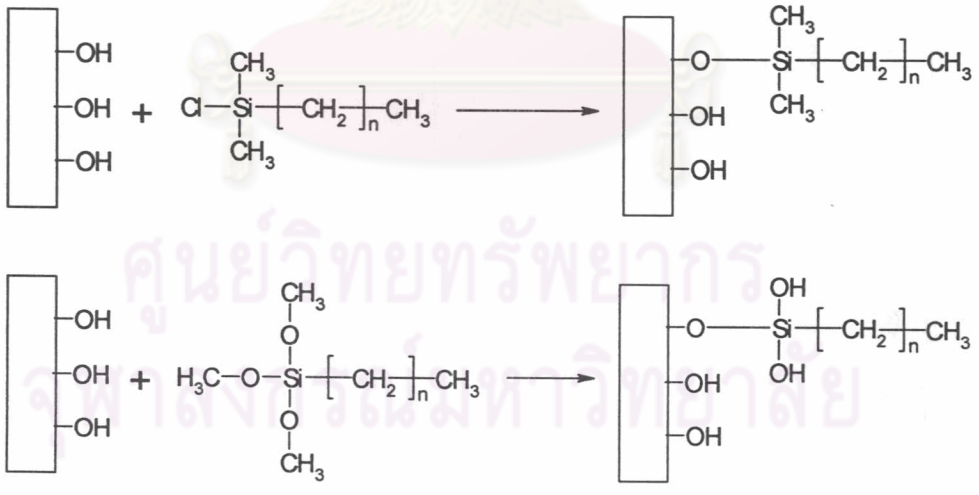

They both will react to the free –OH in the clay which locate at both an edge of the clay and the defect of the clay surface.

The XRD pattern of the OTMS-clay and ODCS-clay are shown in the Figure 4.24 and 4.25. In case of OTMS, there is a slight increased in the d-spacing.

The OTMS-clay shows slight increased in the d-spacing from the Na-clay (can not detect the top of peak). An increased in the d-spacing of about 1.4 Å was observed when the clay is reacted with ODCS. This changed is believed to be originated from the changed of the water content within the clay, not from the surfactant.

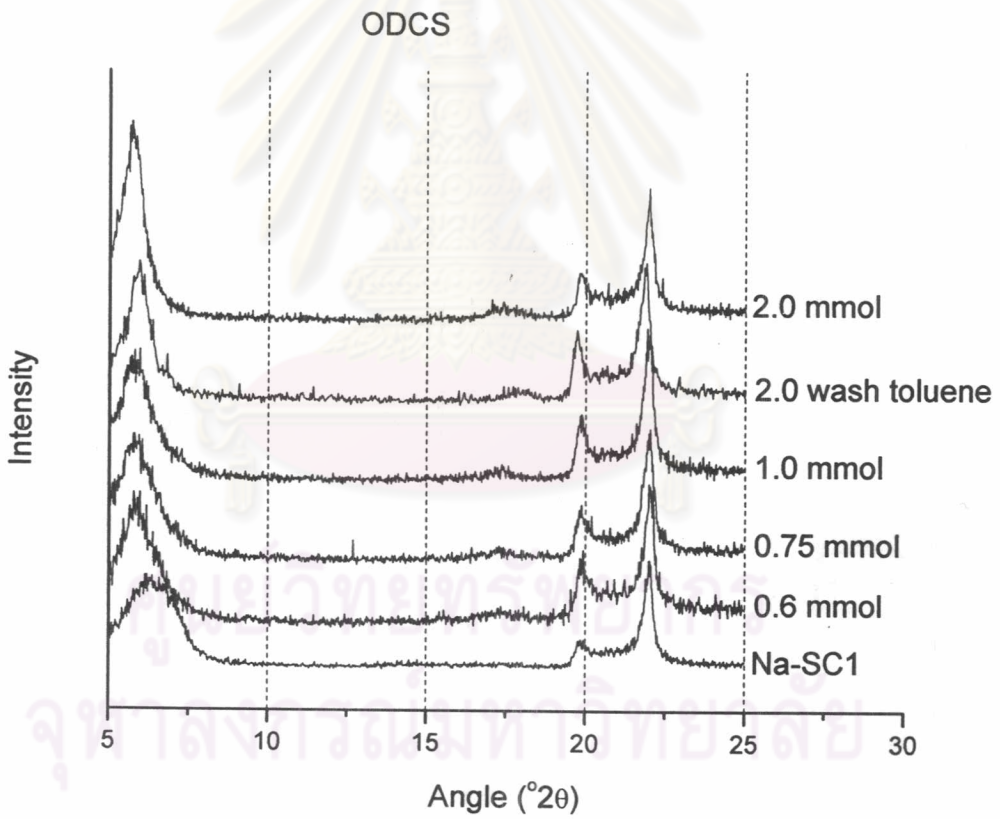

Figure 4.24 XRD pattern of Na-SC1 reacted to ODCS

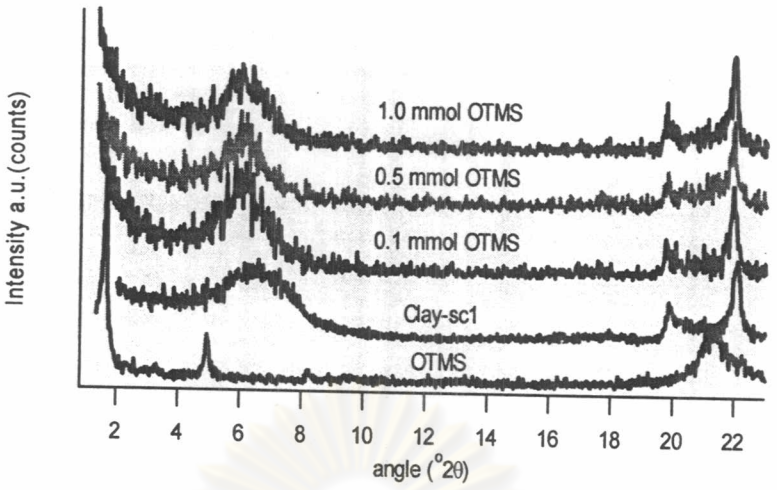

Figure 4.25 XRD pattern of Na-SC1 reacted to ODCS

The samples were characterized by FTIR in order to confirm the existence of the ODCS in the clay. The peak at 1200, 2850, and 2923 cm^{-1} presents the vibration of CH_2 and CH_3 see in Table 4.10. This evidence is a key supporting the interaction between the silane and the clay. The height of peak is increased as a function of the concentration loading as shown in Figure 4.26 and 4.27. This indicates that more of the ODCS are presenting in the clay. Both the XRD and the FTIR led to the conclusion that the ODCS is reacting mostly with OH group on the edge of the clay. The reaction is not very efficient as can be seen from the intensity of the $-CH_2$ (st).

Table 4.10 Summery of FTIR data for octadecyl dimethylchlorosilane and octadecyl trimethoxy silane.

Wave number (cm-1)	Functional group	Octadecyl trimethoxysilane (cm-1)	Octadecyl dimethylchlorosilane (cm-1)
2923	CH3(st)	2920	2926
2850, 1200	CH2(asym.st.)	2850, 1200	2852, 1201
1460	CH2(bending)	1460	-
1130-1000	SiOSi	1090,1040	1093,1039
860	SiCH3	-	850
3700-3400	MOH	3630	3630
3400, 3250, 1640	Water-hydrogen bond	3400, 3250, 1640	3400, 3250, 1640

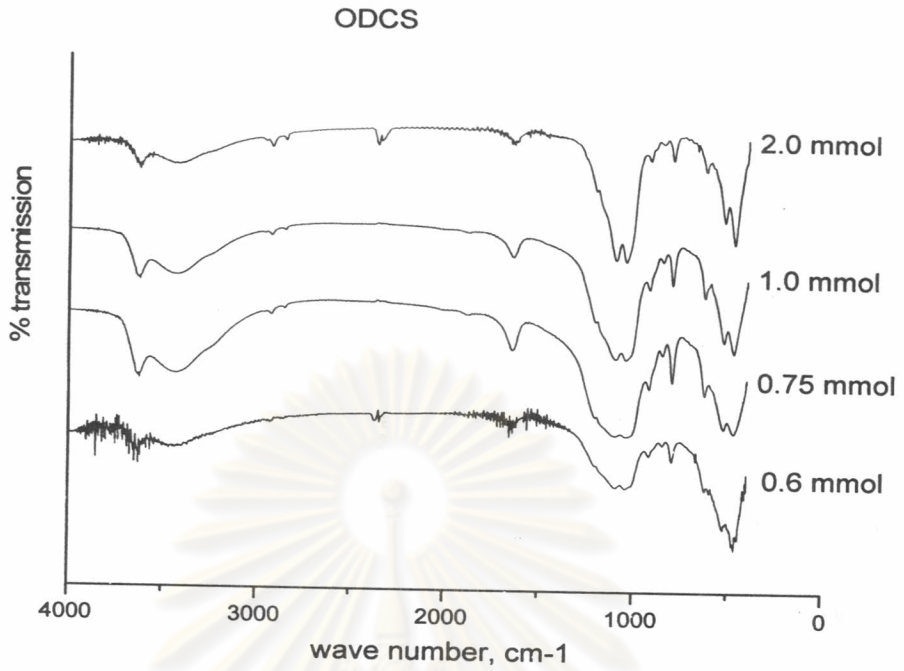

Figure 4.26 FTIR spectrum of octadecyldimethylchlorosilane with Na-clay

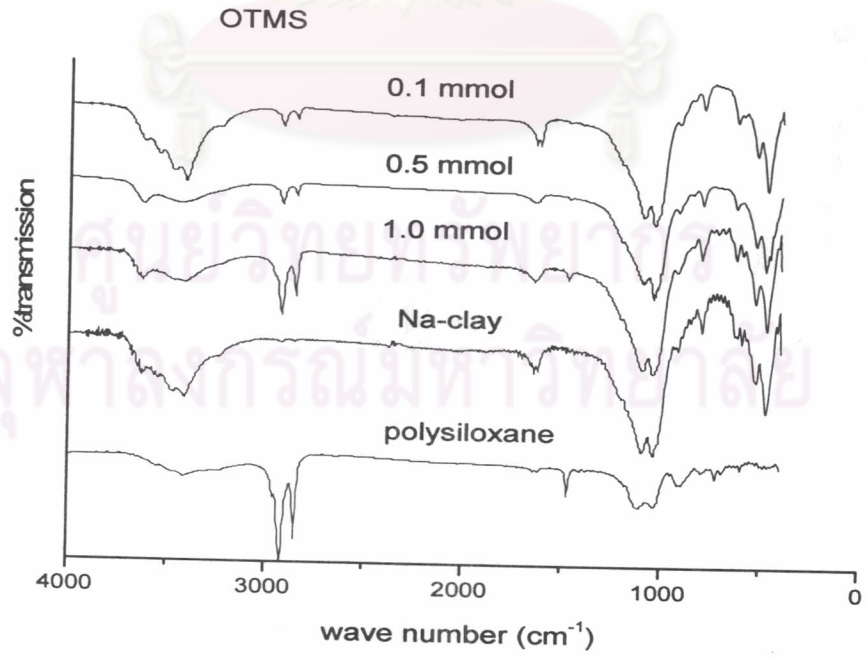

Figure 4.27 FTIR spectrum of octadecyltrimethoxysilane with Na-clay

The treatment was done in the case of OTMS to test on an effect of the reaction site. No changed in the interlayer spacing was observed. Again FTIR was used to clarify the existence of OTMS molecule. The peak between 3400-3700 cm^{-1} of the Na-clay is decreased slightly after reacting with silane, it means the M-OH , such as Al-OH or Si-OH, was changed to be Al-O-Si. An increased in the intensity of the peak at 1000-1100 cm^{-1} was observed. OTMS shows a very strong increased in the CH_2 intensity as the amount of the OTMS loading was increased. This can be explained by the available reactive sites on OTMS molecule. The possibility of OTMS undergoes self polymerization to form polysiloxane cannot be excluded. This may be lead to a drastic changed in the amount of the OTMS observed in the treated organoclay.

Table 4.11 The weight loss comparison of octadecyl dimethyl chloro silane and octadecyl trimethoxy silane.

Concentration (mmol/g)	Weight loss (%)	
	OTMS	ODCS
0.5	19.4	14.3
1.0	25.4	14.2
2.0	24.2	16.7

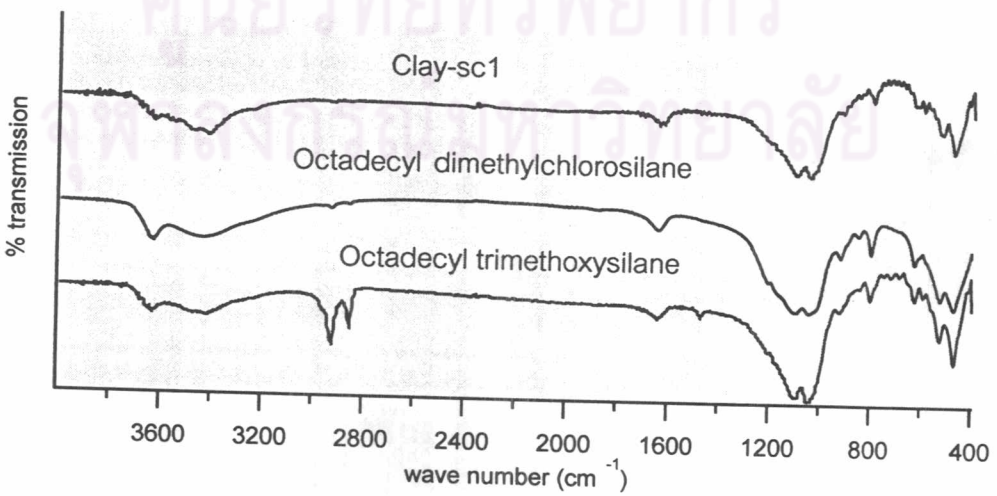

Figure 4.28 FTIR spectra of Na-clay reacted with ODCS and OTMS at 1.0 mmol

The rheology of Na-clay and modifying clay had been investigated by viscometer.

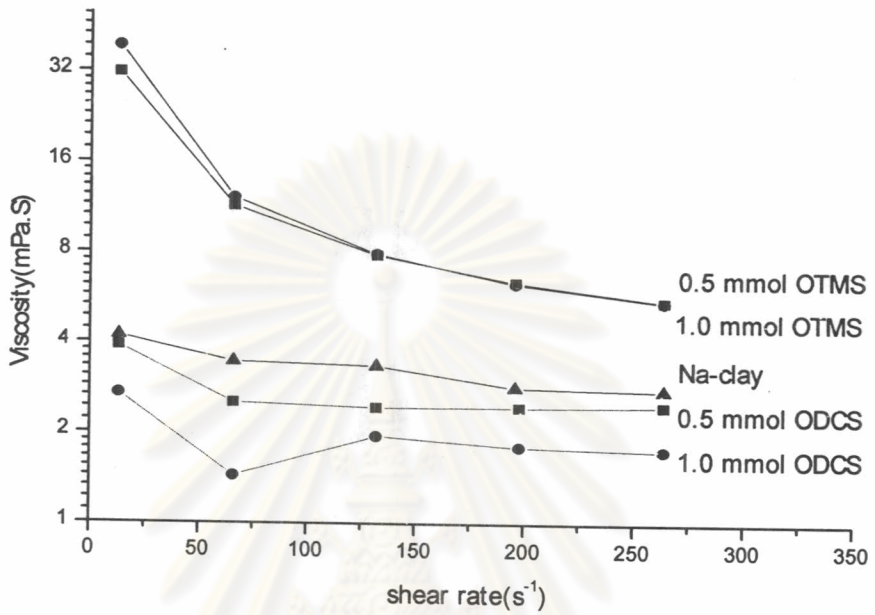

Figure 4.29 Plot of viscosity vs shear rate of Na-clay and modifying clay

The OTMS was chosen for this study in order to avoid the effect of the interaction in the interlayer. Therefore organoclay D18 and organiclay D18 shielded with OTMS dispersing in toluene 5 and 10 %W/V were used to study their rheological behavior. The viscosity of 5 %W/V organiclay D18 with OTMS at constant shear rate (13.2 s^{-1}) has shown thixotopic behavior, their viscosity depending on time as shown in Figure 4.29 and represent flow behavior type shear thinning at 10%W/V in Figure 4.30 when increasing shear rate. However at high solid content, the effect of edge shielding was not significant. Both of modifying clay had shown the flow behavior as pseudoplastic with yield point in Figure 4.31 and 4.32. This phenomenon can be explain by the formation of clay in suspension, the interaction between particles has been decrease as a result of electrostatic force at the edge interference by OTMS, just only the London force held the particle together.

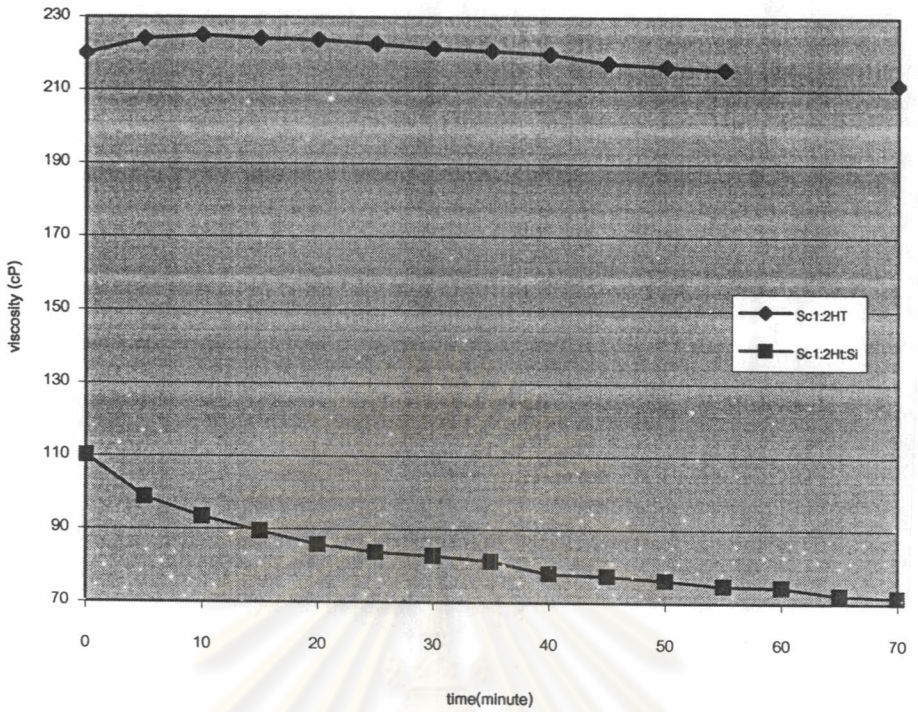

Figure 4.30 The viscosity of organiclay D18 with OTMS at constant shear rate.

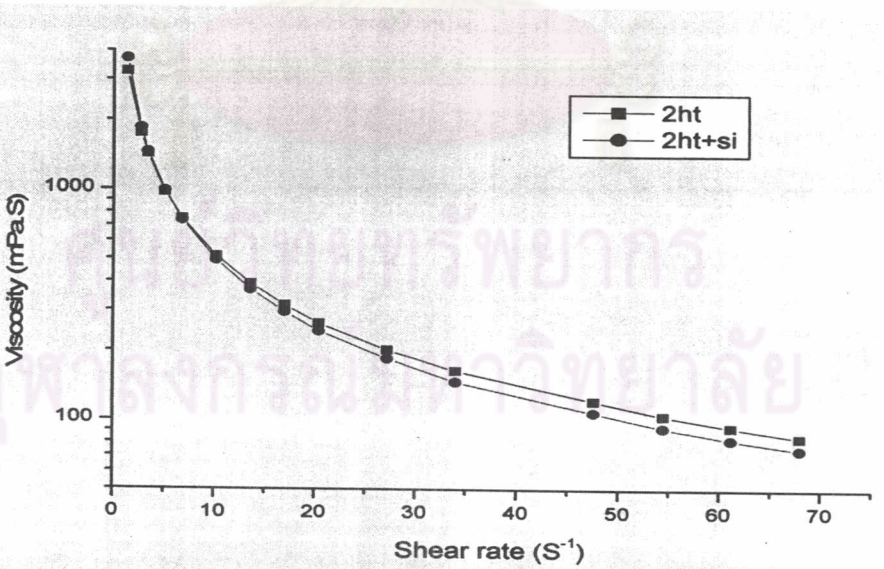

Figure 4.31 The relationship between viscosity and shear rate of modifying clay

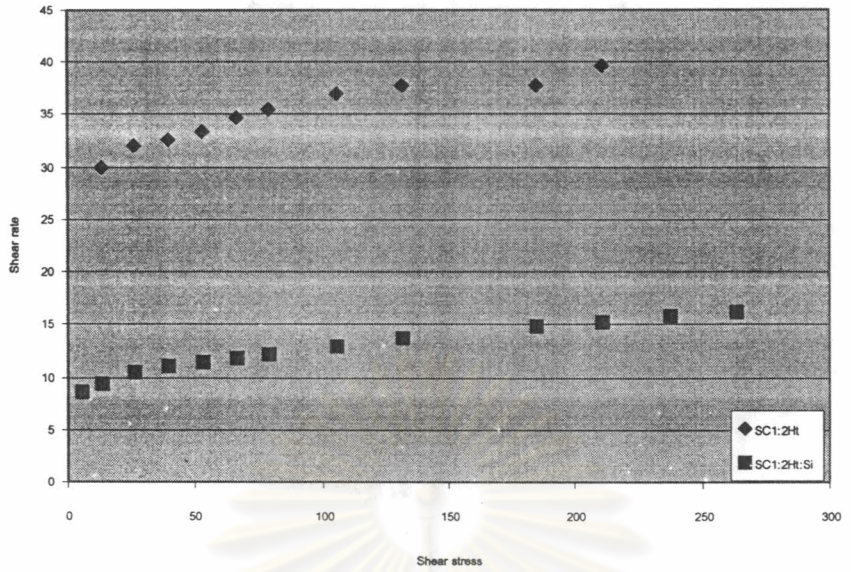

Figure 4.32 Dependence of shear rate on shear stress for modifying clay

4.4 Polymer-clay nanocomposite preparation and characterization

4.4.1 In situ polymerization of polymer-clay nanocomposite

The modifying clay 2.0 mmol D18, both with the edge shielding and non shielding, were used for a preparation of polystyrene clay nanocomposites by in situ intercalative polymerization. 2.0%wt of the organoclay was dispersed in styrene monomer. The XRD pattern of the resulting nancocomposites showed a shoulder at the same position for both organoclay. (See Figure 4.33) This result indicates that polystyrene can be intercalated into the clay layer to form nanocomposite. The clay layer still remains stack together but the d_{001}-spacing can not be clearly detected as a result of the deterioration of the stacking. The formation of nancomposites can be further confirmed by TEM, as shown in Figure 4.34 and 4.35. The micrographes show that there is a present of the organoclay primary particle mixed with an exfoliated nancomposites. On the other hand, the tactoids are still present in the sample and it consists of at least 10 layers of clay stack together. In Figure 4.35 shows the interlayer spacing is around 3-4 nm which corresponding to XRD results.

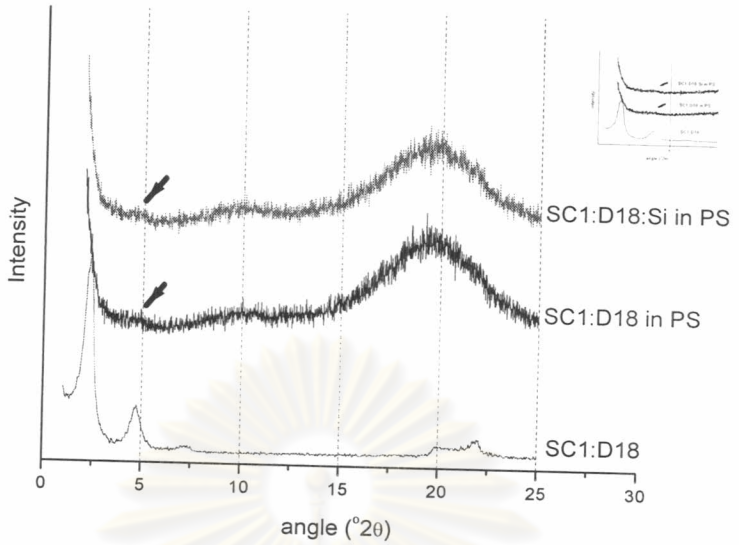

Figure 4.33 XRD pattern of 2 wt% organoclay in PS composite

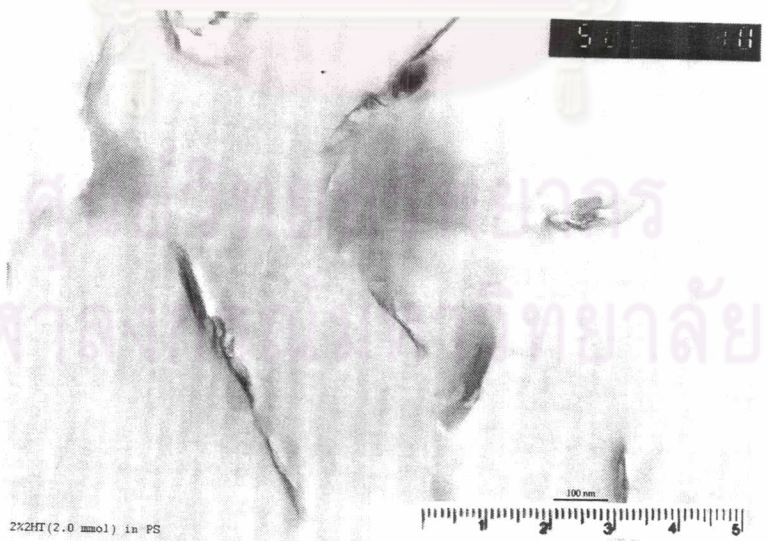

Figure 4.34 TEM micrograph of polymer clay nanocomposite at 99,000X

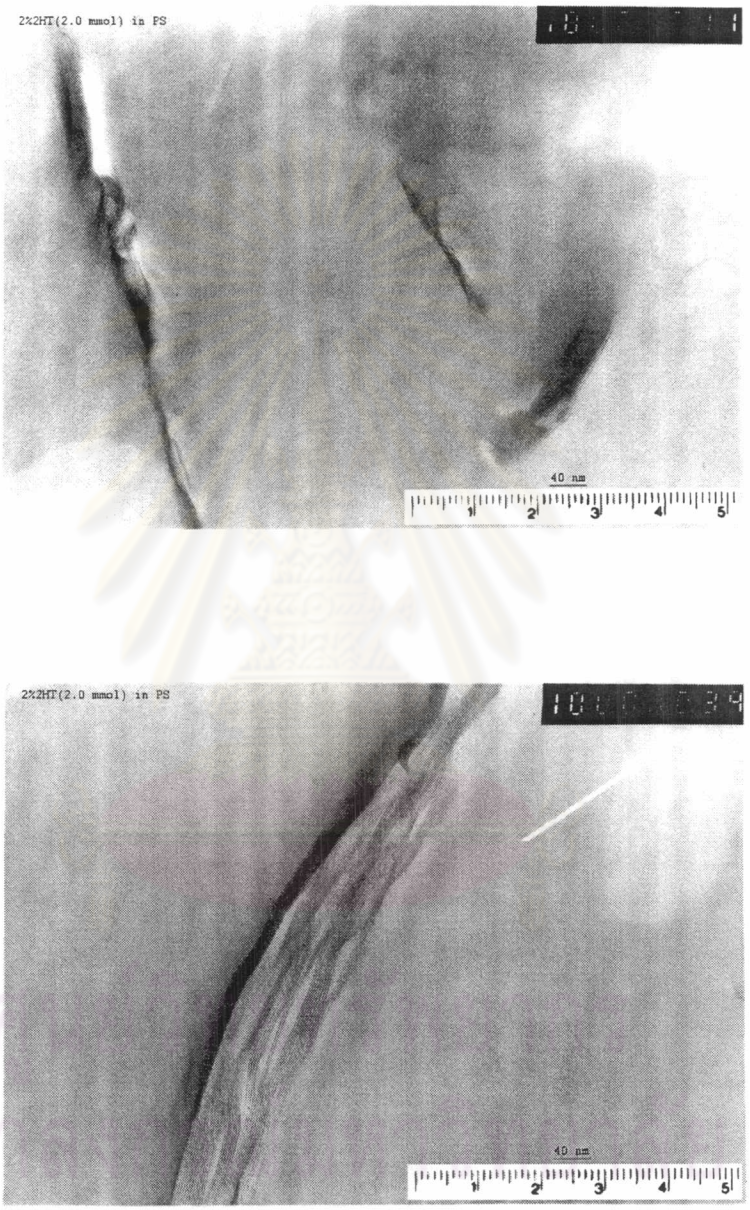

Figure 4.35 TEM micrograph of polymer clay nanocomposite at 150,000X

The effect of percent solid loading was studied by XRD at 2, 3 and 5% by weight of polystyrene. The intensity of diffractogram at around 3-5 $^{o}2\theta$ increased when the amount of organoclay loading is increased. This implies that the formation of nanocomposite is depending upon the volume content of organoclay as shows in Figure 4.36. At lower loading the styrene can penetrate into the clay layer, as a result of peak position of XRD diffractogram shift to the left hand.

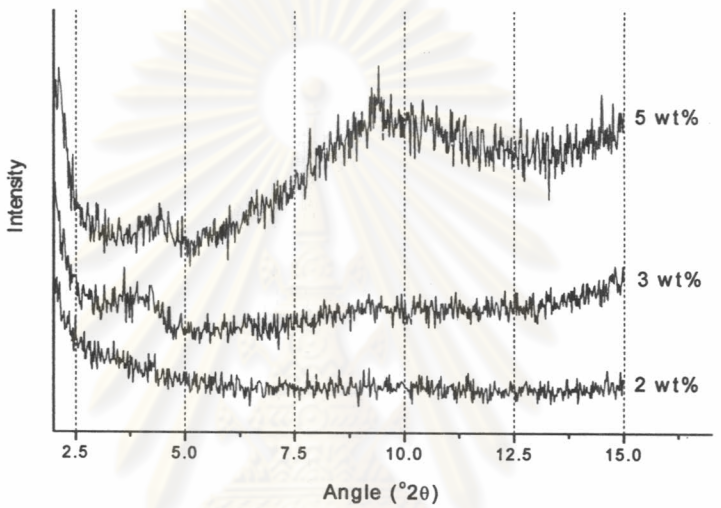

Figure 4.36 XRD pattern of organoclay D18 (2.0 mmol) in PS at various contents

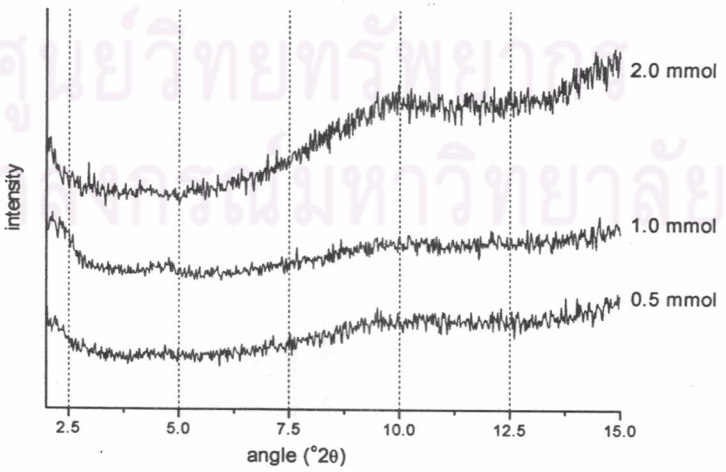

Figure 4.37 XRD pattern of different surface coverage of organoclay D18 in PS by in situ polymerization

At the same solid loading content (2%wt), the different surface coverage of organoclay has an effect to the nanocomposite conformation. At the low surface coverage the dispersion of the organoclay in styrene does not completely disperse the organoclay,. As a result, both transparent and opaque were observed for the suspension. Surprisingly the XRD peak cannot be detected in this sample (Figure 4.37). This implies that the clay surface coverage has no effect on the formation of polystyrene-clay nanocomposite which prepared by in situ polymerization.

4.4.2 Melt-intercalation of polystyrene-clay nanocomposites

The main objective of this part is to study an effect of the organoclay surface coverage on the formation of the polystyrene-clay nancomposites by melt intercalation. Polystyrene (GP110) was mixed with organoclay D18 at 180 °C for 10 minutes at the mixing speed of 50 rpm. The formation of polymer-clay nanocomposite was detected by XRD as shown in Figure 4.38 nanocomposites. At the low surface coverage, 0.5 CEC, the polystyrene shows an increased in the interlayer spacing. While at the higher surface coverage, the polystyrene forms only a conventional composite.

The formation of the compsites was confirmed by TEM picture from Figure 4.39-4.44. The organoclay at high surface coverage (2.0 mmol) has shown a good distribution in the polystyrene matrix at low magnification. The clay particle can be disaggregated as a primary particle, but also stacked together as shown in Figure 4.40. The XRD pattern of organoclay (2.0 mmol) D18 in PS by melt processing show sharp XRD peak.

For organoclay at 0.5 and 1.0 mmol of D18, polystyrene penetrated into the interlayer and shown partial exfoliated (Figure 4.45 – 4.53). As a result of the XRD pattern of polystyrene-clay nanocomposite shift to lower angle and broader than the XRD pattern of organoclay.

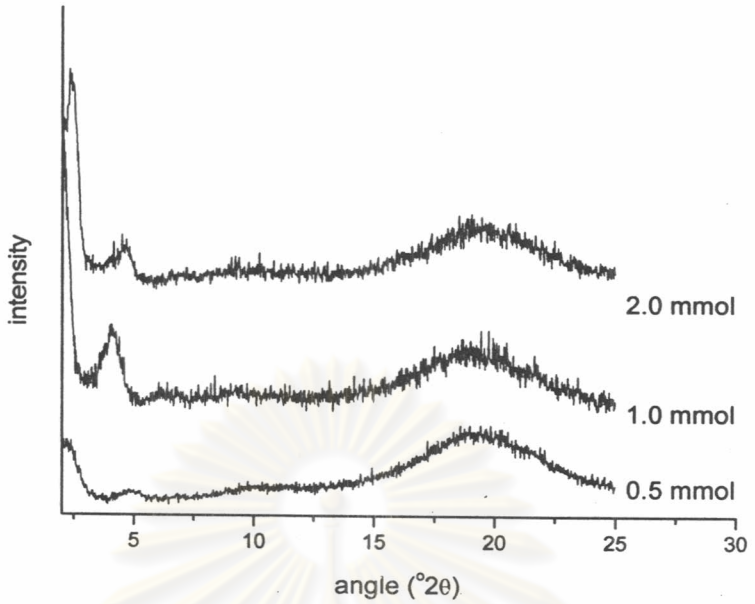

a) Diffractogram of Polystyrene-clay composite

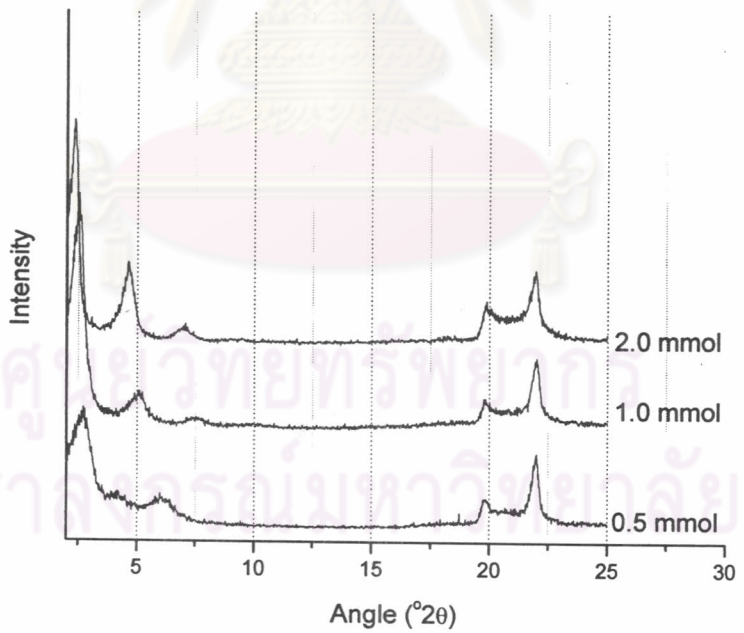

b) Diffractogram of organo-clay (D18)

Figure 4.38 XRD pattern of different surface coverage of organoclay D18 in PS by melt blending

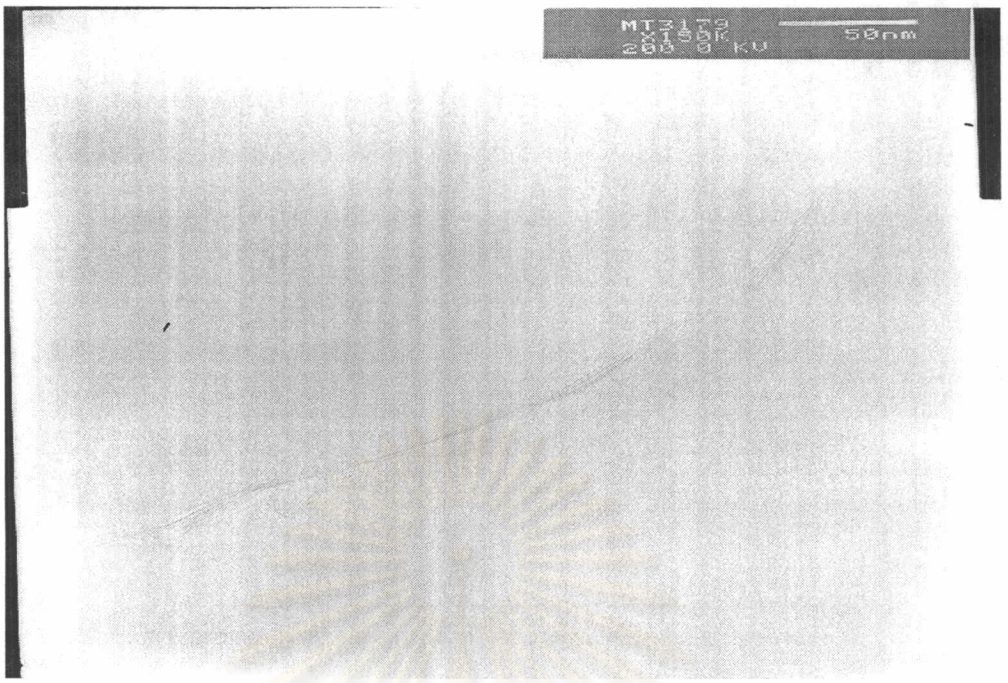

Figure 4.39 Micrograph of PS-(2.0 mmol) D18 composite at 150,000 X

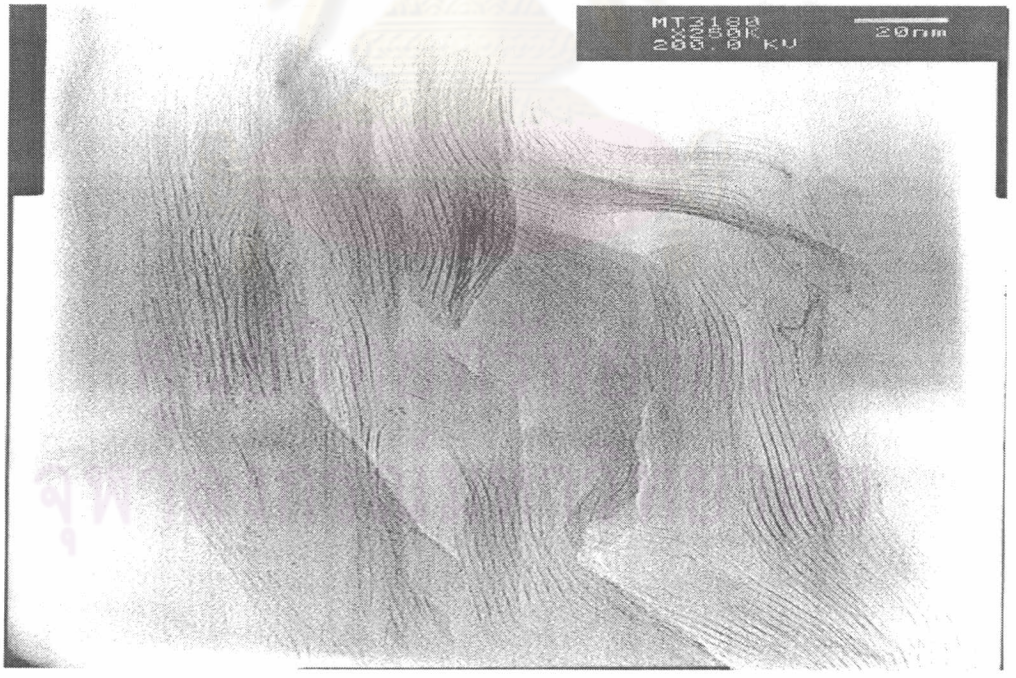

Figure 4.40 Micrograph of PS-(2.0 mmol) D18 composite at 250,000 X

Figure 4.41 Micrograph of PS-(2.0 mmol) D18 composite at 300,000 X

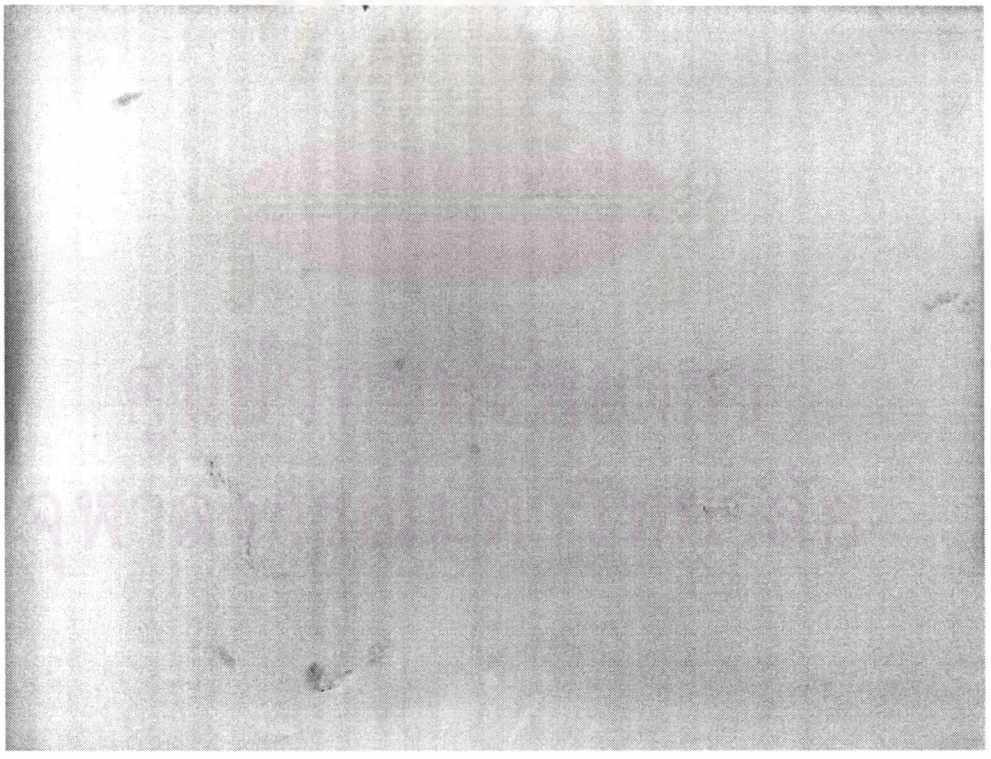

Figure 4.42 Micrograph of PS-(2.0 mmol) D18 composite at 50,000 X

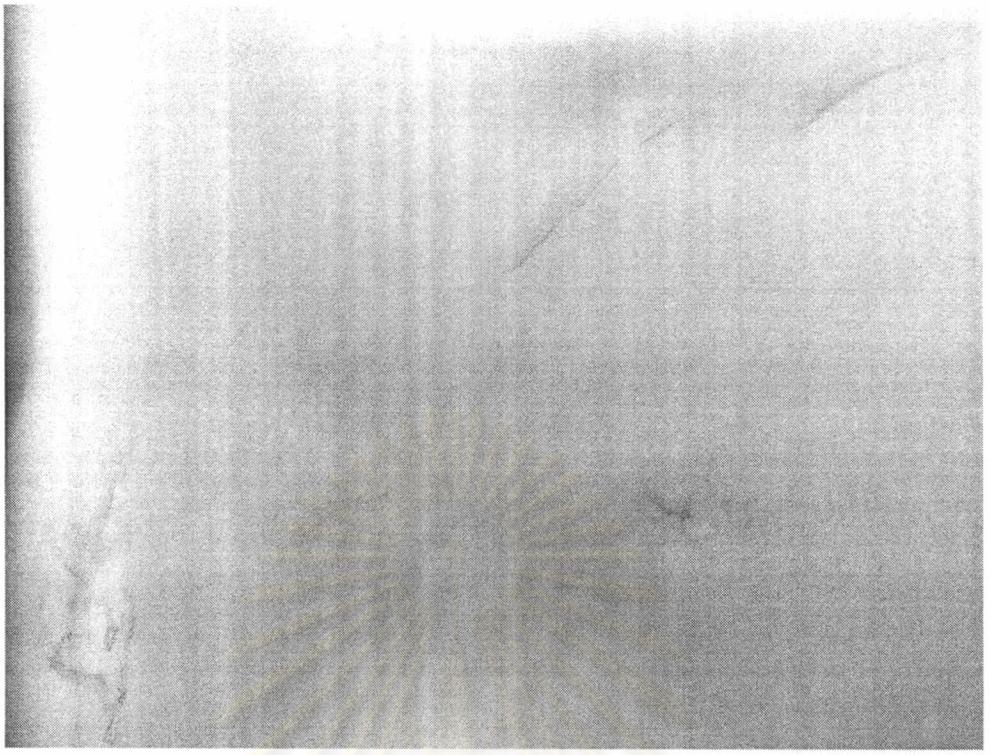

Figure 4.43 Micrograph of PS-(2.0 mmol) D18 composite at 50,000 X

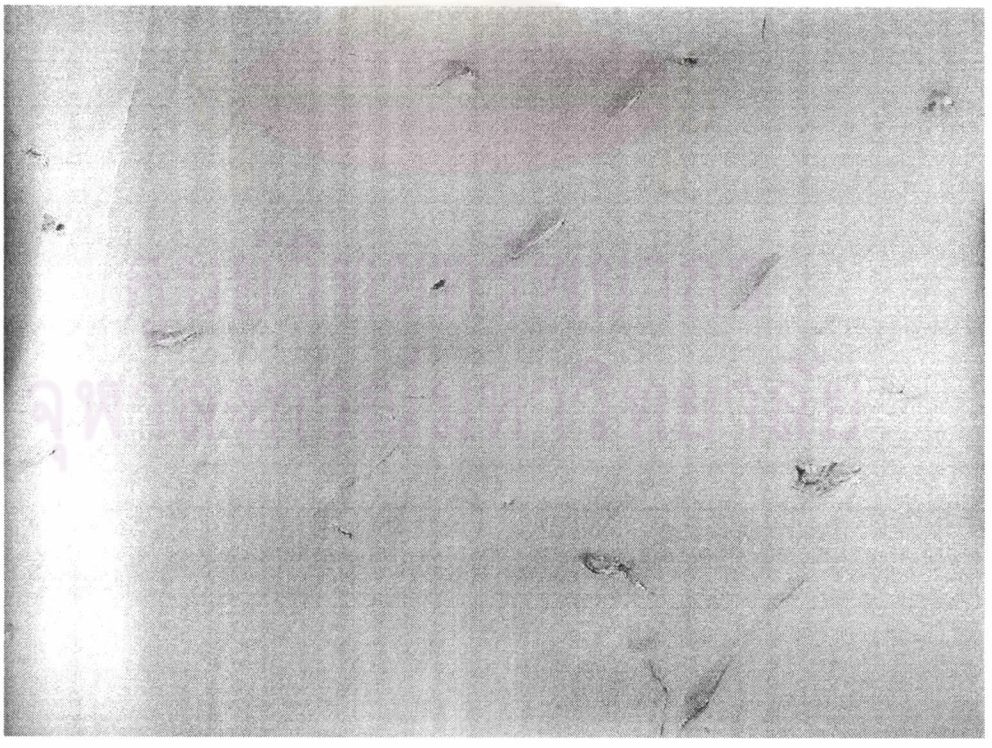

Figure 4.44 Micrograph of PS-(2.0 mmol) D18 composite at 15,000 X

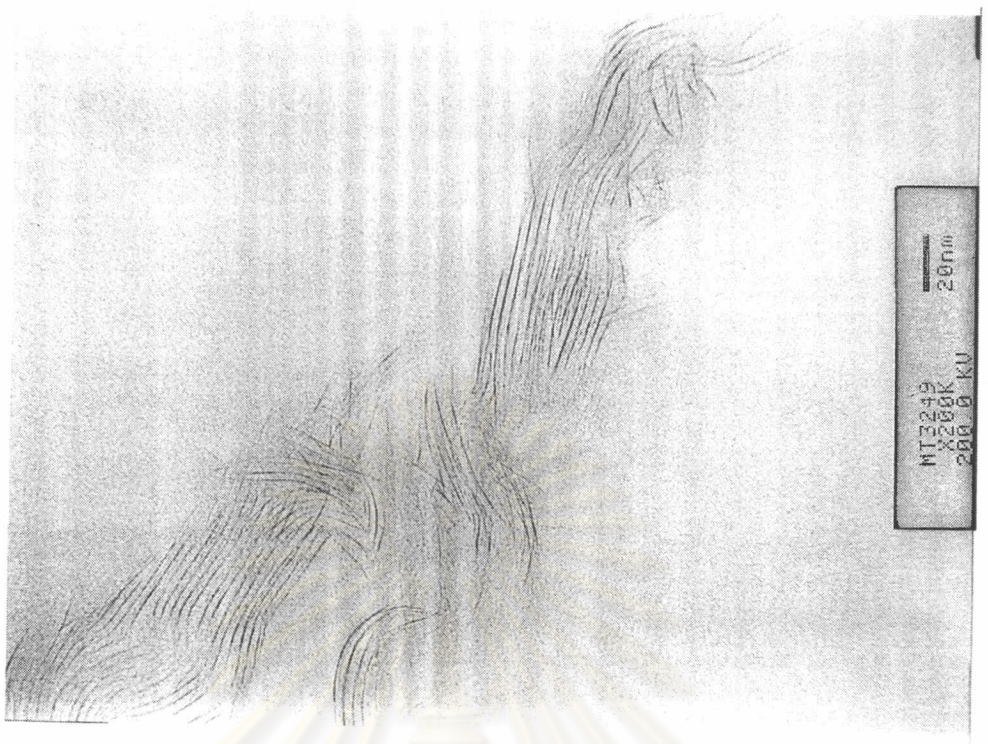

Figure 4.45 Micrograph of PS-(1.0 mmol) D18 composite at 200,000 X

Figure 4.46 Micrograph of PS-(1.0 mmol) D18 composite at 150,000 X

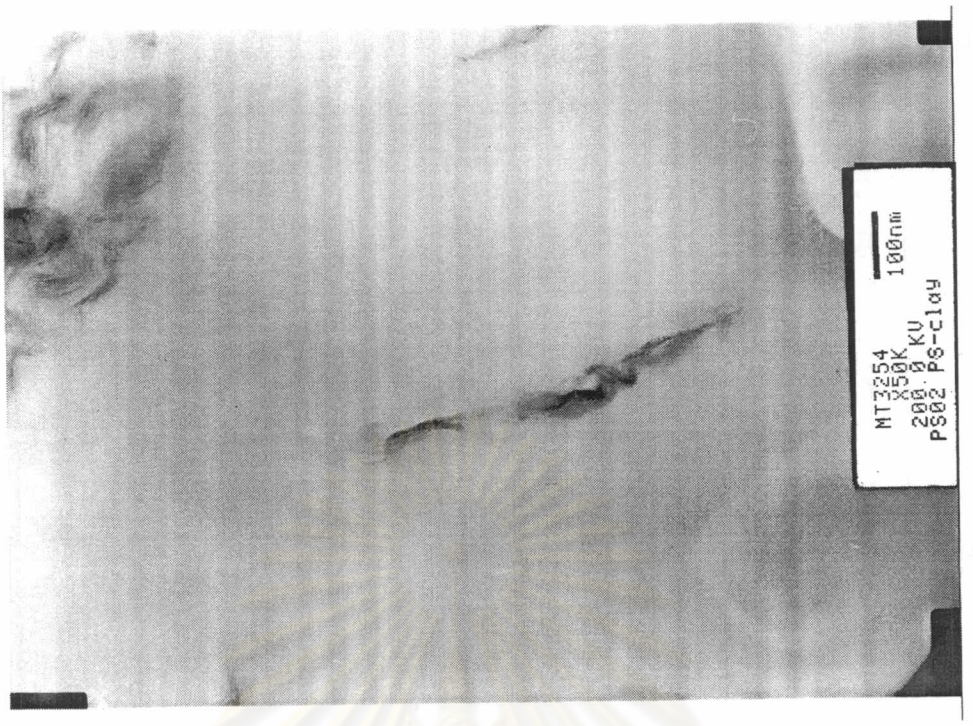

Figure 4.47 Micrograph of PS-(1.0 mmol) D18 composite at 50,000 X

Figure 4.48 Micrograph of PS-(1.0 mmol) D18 composite at 20,000 X

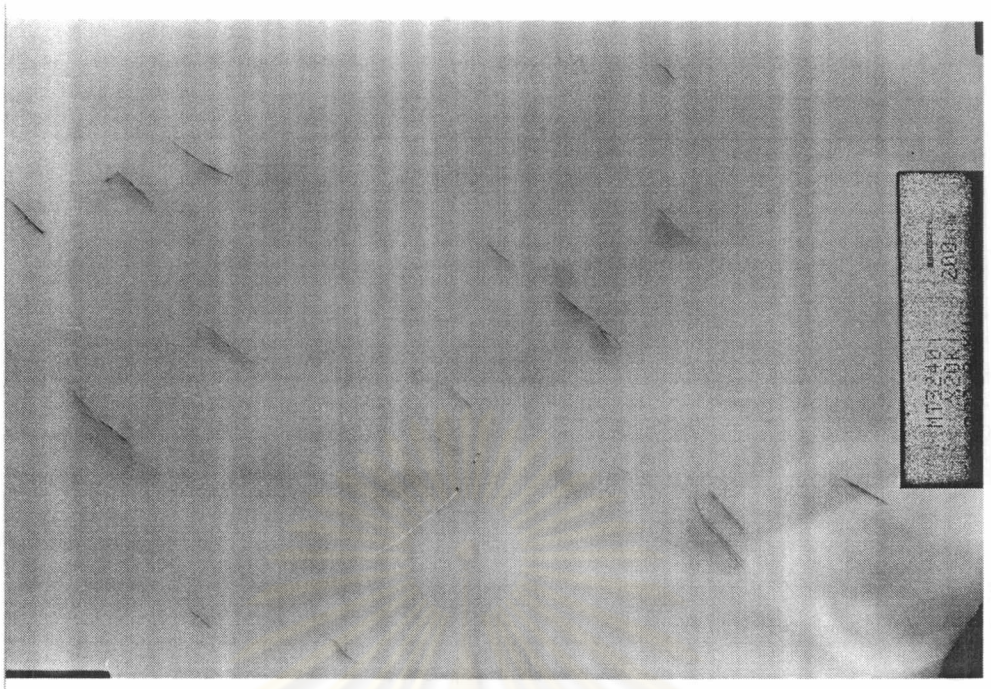

Figure 4.49 Micrograph of PS-(0.5 mmol) D18 composite at 20,000 X

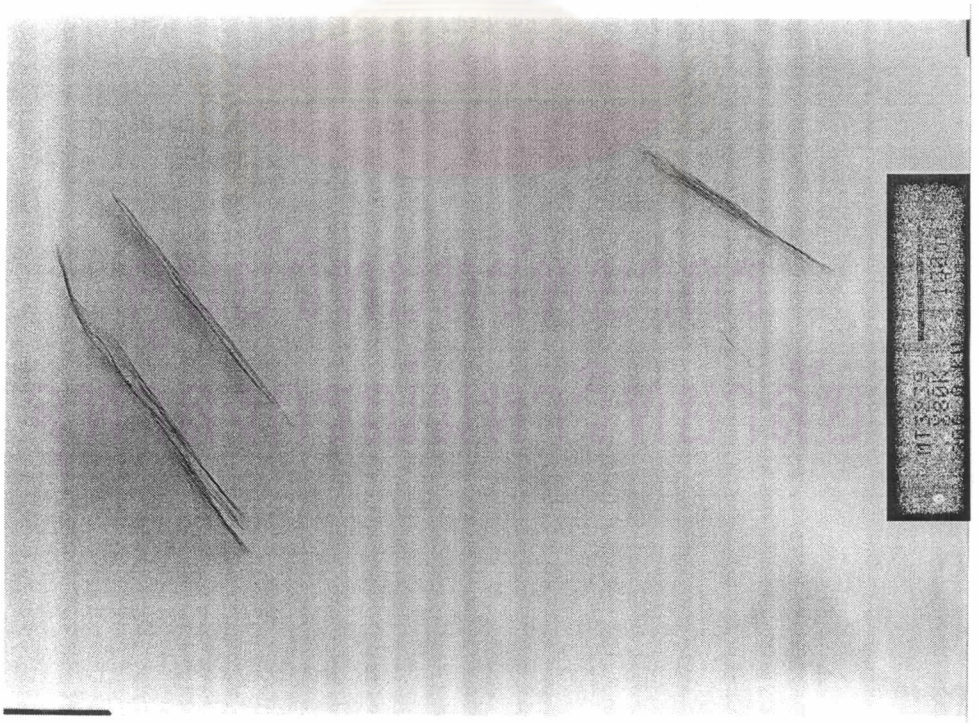

Figure 4.50 Micrograph of PS-(0.5 mmol) D18 composite at 50,000 X

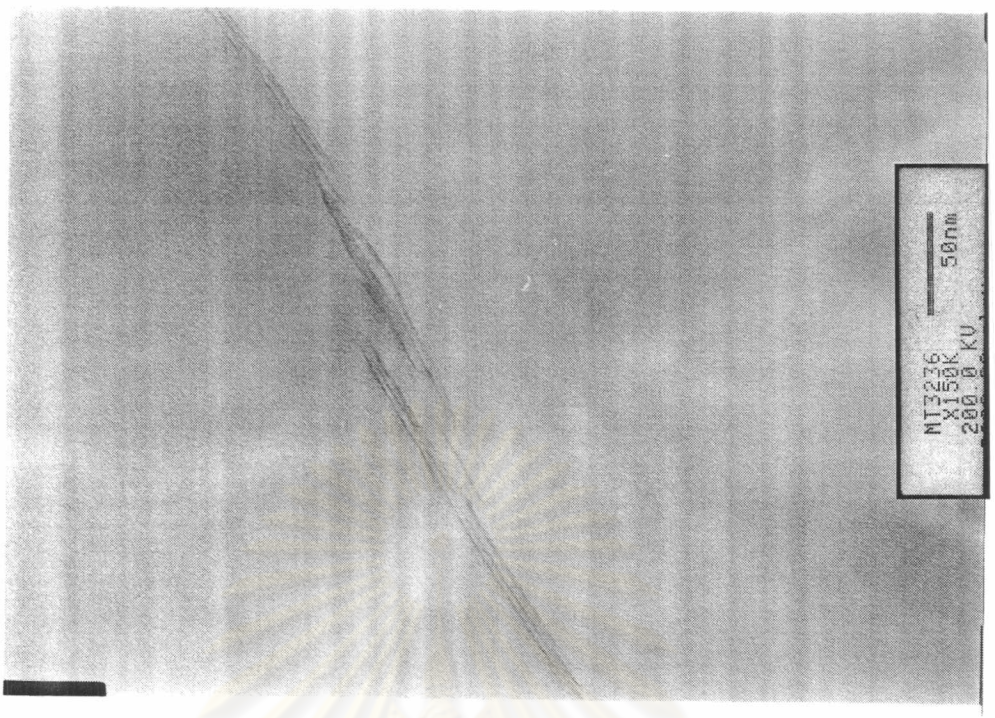

Figure 4.51 Micrograph of PS-(0.5 mmol) D18 composite at 150,000 X

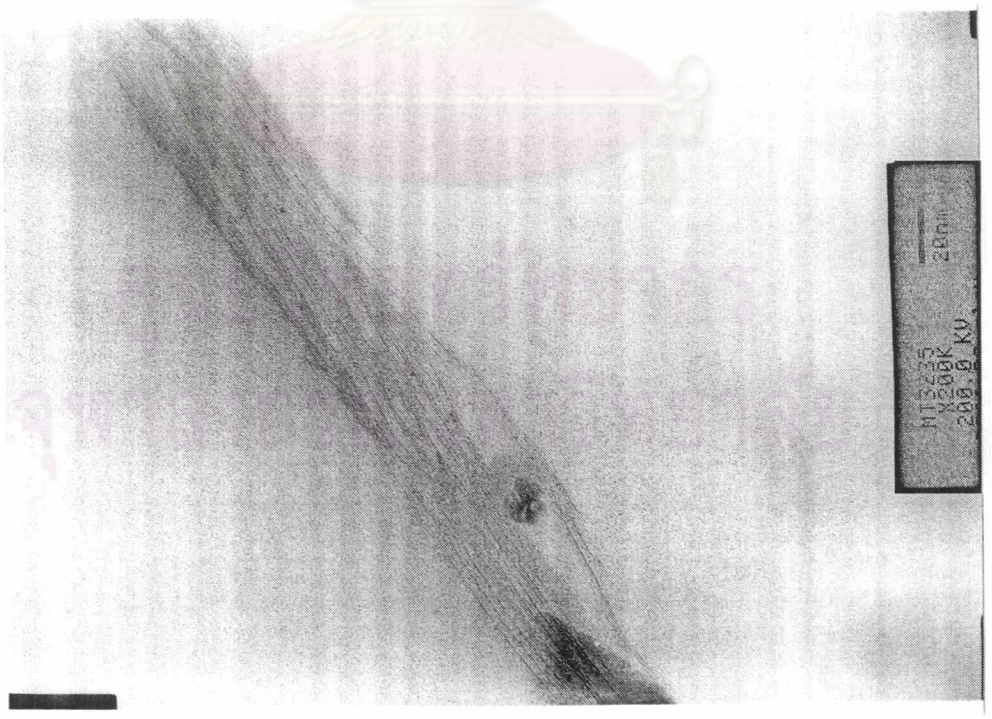

Figure 4.52 Micrograph of PS-(0.5 mmol) D18 composite at 200,000 X

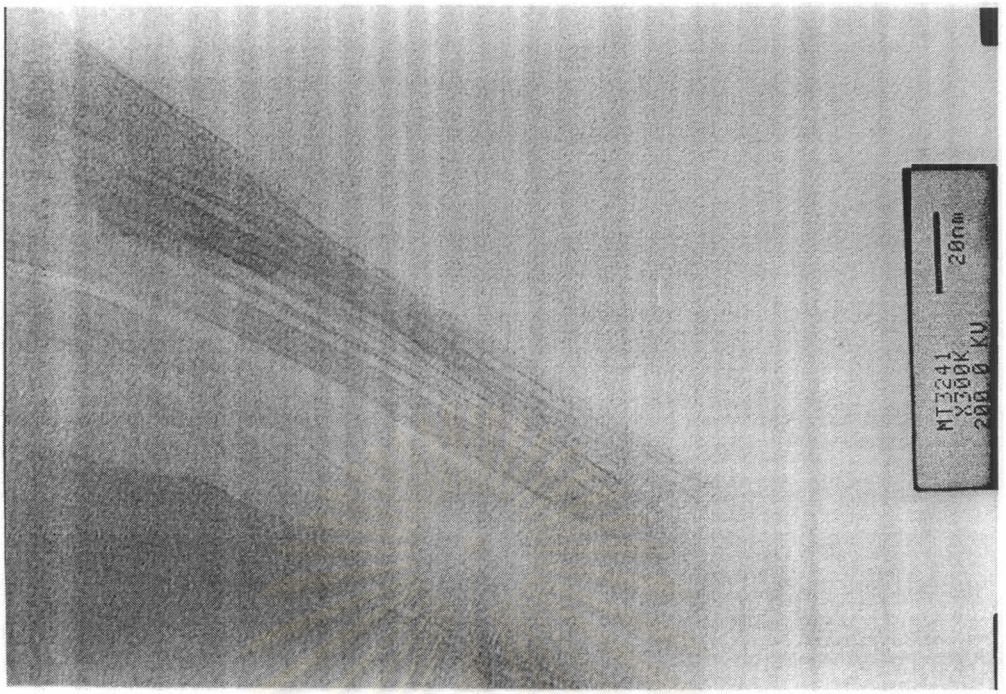

Figure 4.53 Micrograph of PS-(0.5 mmol) D18 composite at 300,000 X

4.4.3 Melt-intercalation of nylon6-clay nanocomposites

This experiment was done in order to elucidate an effect of clay surface treatment on the formation of polymer-clay nanocomposite by melt intercalation. Three major types of the organoclay were used in this study. The first two samples are the organoclay which possess the same surface chemistry but a major difference is their surface coverage. The third system consists of a surfactant with a more polar group which rendering the more polar surface. This was done in order to monitor an effect of the organoclay's surface chemistry to the intercalation process.

They are 2.0 mol-D18 and 0.5 mol-D18 where total amount of the surfactant in the organoclay is at 53.3% and 31.2%, respectively. The interlayer spacing of both organoclay is at 38.4 Å and 28.9 Å. The higher spacing corresponds to a tighter packing of the interlayer surfactant (Figure 5.54) which is originated from a less tilting of the surfactant molecule with respect to the clay surface [Lee S.Y., 2002].

The organoclay with a high surface coverage of the 2.0 mol-D18 does not exhibit any changed in the interlayer spacing in an extruded sample. Figure 4.55 shows that both the position and the intensity of the peak remain almost the same as in the organoclay. This mans that the nylon6 does not intercalate into the interlayer spacing of the organoclay. This may be due to a poor compatibility between the organoclay surface and the nylon6. A sharp diffraction maximum along with its higher order diffraction peak are still observed at all level of organoclay loading. This suggests that organoclay primary particle was not disturbed by the extruded process as evidenced by the XRD pattern.

Beside the surface chemistry there might be the high density packing of the surfactant responsible as well. The surfactant functionality is the alkyl-terminated which relatively non-polar compared to nylon6. This final morphology is categorized as the conventional composites or micro composites [Kornmann X., 2003]. This is resulting in a restricted intercalation of the polymer chain into the clay surface.

An improvement in the dispersion was observed in the case of 0.5mol-D18 where the clay possesses an incomplete coverage by the surfactant. The higher order peak, which is an indication of the crystallographic order of the organoclay stacking, cannot be observed in this case. The XRD pattern (Figure 5.56) shows that the clay stacking is disintegrated. The peak which was observed in the original organoclay is gradually transformed into a shoulder along with the expansion of the interlayer spacing. It may be due to the nature of a polar structure of nylon6 which prefers to wet on the organoclay's surface.

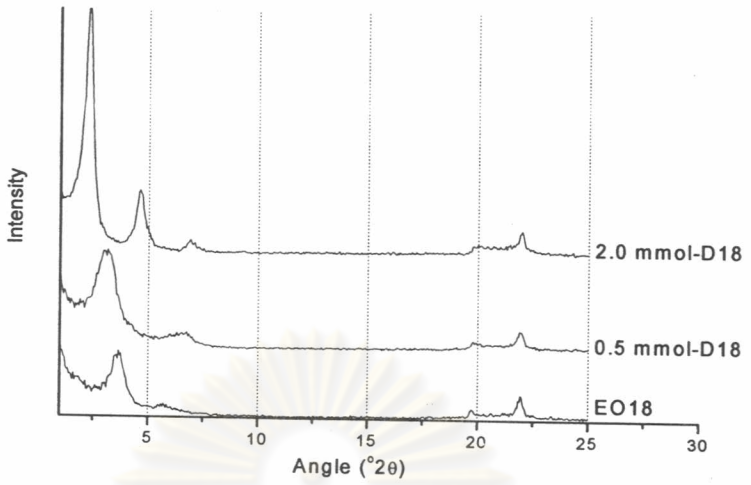

Figure 4.54 XRD of organoclay used in this study.

In the case where a more polar surfactant EO18 was employed, the organoclay shows an improved dispersion over D18 counterpart. As evidenced by a transformation of the small angle peak into a shoulder. The interlayer spacing is also increased from 13.4 Ang to 24.2 Ang. These are an indication for a delaminating of the organoclay into a smaller stack which disperses in the polymer matrix. At the higher organoclay loading, no build up of the higher stacking organoclay was observed. The shoulder appears a little more prominent at 5% organoclay loading due to an increased in the amount of the clay content within the sample (Figure 4.57). The interlayer spacing still remains at the same position. This supports the hypothesis that the wetting is promoted via the treatment of the EO18 onto the clay surface.

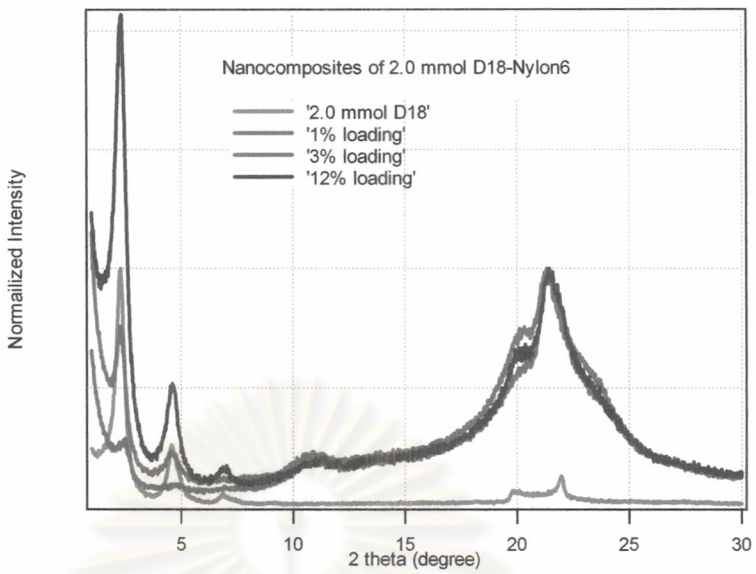

Figure 4.55 XRD of 2.0mmol-D18-nylon6 nanocomposites at 1%, 3% and 12% organoclay loading.

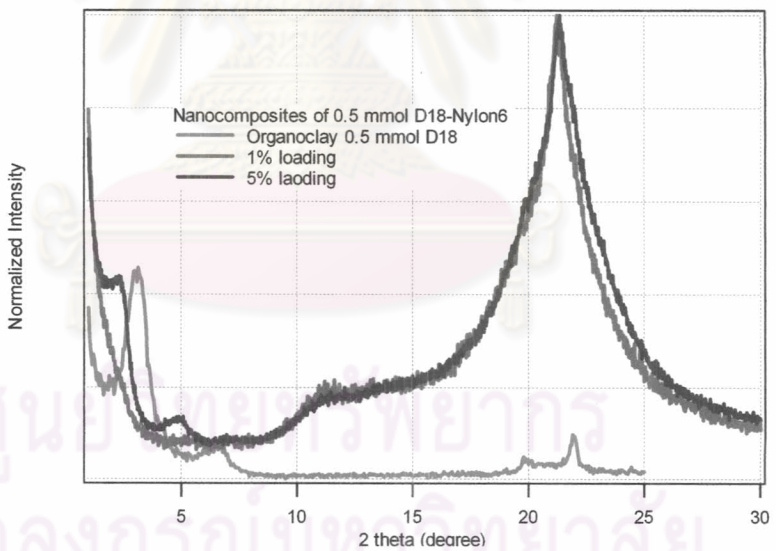

Figure 4.56 XRD of 0.5mmol-D18-nylon6 nanocomposites at 1% and 5% organoclay loading.

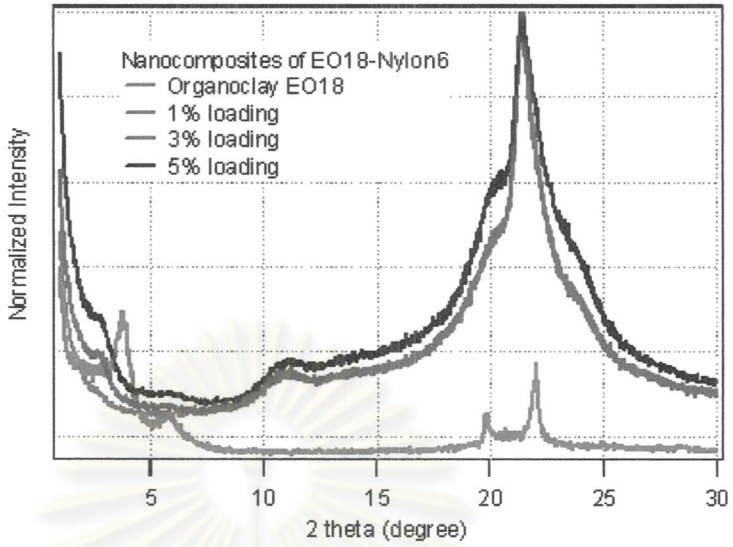

Figure 4.57 XRD of EO18-nylon6 nanocomposites at 1%, 3%, and 5% organoclay loading.